AFFDL-TR-77-54

(2)

BC

SIMULATED LIGHTNING TEST ON THE NAVY AIRBORNE LIGHT OPTICAL FIBER TECHNOLOGY (ALOFT) A-7 AIRCRAFT

JEROME T. DIJAK, CAPTAIN, USAF

ELECTROMAGNETIC HAZARDS GROUP
SURVIVABILITY/VULNERABILITY BRANCH
VEHICLE EQUIPMENT DIVISION

JUNE 1977

TECHNICAL REPORT AFFDL-TR-77-54
Final Report for Period 1-31 August 1976

Approved for public release; distribution unlimited.

AIR FORCE FLIGHT DYNAMICS LABORATORY
AIR FORCE WRIGHT AERONAUTICAL LABORATORIES
AIR FORCE SYSTEMS COMMAND
WRIGHT-PATTERSON AIR FORCE BASE, OHIO 45433

NOTICE

When Government drawings, specifications, or other data are used for any purpose other than in connection with a definitely related Government procurement operation, the United States Government thereby incurs no responsibility nor any obligation whatsoever; and the fact that the government may have formulated, furnished, or in any way supplied the said drawings, specifications, or other data, is not to be regarded by implication or otherwise as in any manner licensing the holder or any other person or corporation, or conveying any rights or permission to manufacture, use, or sell any patented invention that may in any way be related thereto.

This report has been reviewed by the Information Office (OI) and is releasable to the National Technical Information Service (NTIS). At NTIS, it will be available to the general public, including foreign nations.

This technical report has been reviewed and is approved for publication.

Jerome T Dijak

Jerome T. Dijak, Captain, USAF
Atmospheric Electricity Engineer

FOR THE COMMANDER

AMBROSE B. NUTT, Director
Vehicle Equipment Division

Copies of this report should not be returned unless return is required by security considerations, contractual obligations, or notice on a specific document.

AIR FORCE/56780/17 October 1977 — 300

UNCLASSIFIED

SECURITY CLASSIFICATION OF THIS PAGE *(When Data Entered)*

REPORT DOCUMENTATION PAGE

READ INSTRUCTIONS BEFORE COMPLETING FORM

1. REPORT NUMBER: AFFDL-TR-77-54	2. GOVT ACCESSION NO.
3. RECIPIENT'S CATALOG NUMBER	
4. TITLE *(and Subtitle)*: SIMULATED LIGHTNING TEST ON THE NAVY AIRBORNE LIGHT OPTICAL FIBER TECHNOLOGY (ALOFT) A-7 AIRCRAFT.	5. TYPE OF REPORT & PERIOD COVERED: Final 1-31 August 1976
	6. PERFORMING ORG. REPORT NUMBER
7. AUTHOR(s): Jerome T. Dijak, Captain, USAF	8. CONTRACT OR GRANT NUMBER(s)
9. PERFORMING ORGANIZATION NAME AND ADDRESS: Electromagnetic Hazards Group/FESL, Air Force Flight Dynamics Laboratory, Wright-Patterson AFB, OHIO 45433	10. PROGRAM ELEMENT, PROJECT, TASK AREA & WORK UNIT NUMBERS: 75000300
11. CONTROLLING OFFICE NAME AND ADDRESS: Naval Electronics Laboratory Center, Code 1600, 271 Catalina Blvd, San Diego, California 92152	12. REPORT DATE: June 1977
	13. NUMBER OF PAGES: 87
14. MONITORING AGENCY NAME & ADDRESS *(if different from Controlling Office)*	15. SECURITY CLASS. *(of this report)*: UNCLASSIFIED
	15a. DECLASSIFICATION/DOWNGRADING SCHEDULE

16. DISTRIBUTION STATEMENT *(of this Report)*

Approved for public release; distribution unlimited.

DDC RECEIVED NOV 4 1977 B

17. DISTRIBUTION STATEMENT *(of the abstract entered in Block 20, if different from Report)*

18. SUPPLEMENTARY NOTES

19. KEY WORDS *(Continue on reverse side if necessary and identify by block number)*

Survivability
Lightning
Fiber Optics
ALOFT

20. ABSTRACT *(Continue on reverse side if necessary and identify by block number)*

A simulated lightning test was conducted on the Navy A-7 Airborne Light Optical Fiber Technology (ALOFT) aircraft for the purpose of determining the advantage gained in the substitution of fiber optics data links within the Navigation and Weapons Delivery System over conventional wiring in reducing lightning-induced transients experienced by the Navigation and Weapons Delivery Computer (NWDC). A 1.6 x 50 microsecond double-exponentional pulse of 2000 amperes peak current was used for the lightning simulation. (cont'd)

DD FORM 1 JAN 73 1473 EDITION OF 1 NOV 65 IS OBSOLETE

UNCLASSIFIED

SECURITY CLASSIFICATION OF THIS PAGE *(When Data Entered)*

012070 AB

Transients on three data circuits, one power supply circuit, and two electo-optical circuits were monitored in seven system configurations. The substitution of fiber optics for the signal wiring reduced the induced transients in the data circuits by 85 to 90 per cent over those observed with the hard-wiring in place. Direct electromagnetic coupling of transient energy into the NWDC was found to be only 9 to 16 per cent as great as the combined effects of coupling due to the signal and power wiring. The relative magnitudes of the signal-wiring and power-wiring induced transients were found to vary among the three data circuits.

FOREWORD

This report was prepared by the Survivability/Vulnerability Branch, Vehicle Equipment Division, Air Force Flight Dynamics Laboratory. The experimental program was requested and funded by the Air Systems Program Office, Naval Electronics Laboratory Center, San Diego, California. The test program was conducted during August 1976 at the Naval Air Test Center, Patuxent River, Maryland. The Air Force Project Engineer was Captain Jerome T. Dijak. Project technical support was provided by Technology Scientific Services, Incorporated of Dayton, Ohio.

TABLE OF CONTENTS

TABLE OF CONTENTS (Continued)

TABLE OF CONTENTS (Continued)

LIST OF FIGURES

LIST OF FIGURES (Continued)

LIST OF FIGURES (Continued)

LIST OF TABLES

1. INTRODUCTION

1.1 Background

1.1.1 General. The current trend toward use of more and more sophisticated electronic systems in critical airborne applications has caused a heightened awareness of the threat represented by lightning strikes to aircraft carrying such systems. It has long been known that voltage transients are produced within aircraft electrical wiring when the vehicle is struck by lightning, but in the past these effects have resulted in relatively minor damage to critical systems onboard.

Now that the electronics systems contain primarily solid-state devices rather than vacuum tubes, the tolerance of these systems to transients has been greatly reduced. Coupled with the advent of mission-critical and flight-critical electronic systems, this problem takes on major proportions.

1.1.2 Fiber Optics. One of the major protection schemes for electrical systems receiving great interest now is that of replacing electrical wiring with fiber optics data links wherever possible to reduce or eliminate lightning and electromagnetic pulse (EMP) susceptibility. To date, systems have been built (the Navy A-7 ALOFT project is one) to demonstrate that a major subsystem can be designed to operate with fiber optics data links, but the quantitative gain in lightning and EMP survivability provided by the use of fiber optics over conventional wiring has not yet been shown. This test program seeks to do just that.

1.1.3 Lightning Energy Coupling. The transient voltages and currents experienced by aircraft avionics systems due to the flow of lightning current through the aircraft's skin and structure can be considered to be coupled into the avionics by three different mechanisms: (1) Electromagnetic induction into the power supply wiring within the aircraft, (2) Electromagnetic induction into the low-level signal wiring within the aircraft, and (3) Electromagnetic induction directly into the device or subsystem. Little information has been available to date on the relative importance of these three mechanisms; this test program also seeks to illuminate this area.

1.1.4 Transient Analysis Testing. The method currently in use for determining the amplitudes and character of induced transients on aircraft is the Transient Analysis Test.[1] This test applies a current pulse (similar to lightning in waveshape, but much lower in peak current) to the aircraft under test, while circuits of interest are monitored to record the transients that are induced. This procedure was used in this program.

1.2 A-7 ALOFT Navigation and Weapons Delivery System

The A-7 ALOFT (Airborne Light Optical Fiber Technology) navigation and weapons delivery system (NWDS) provides a very useful testbed for investigating the effectiveness of fiber optics in reducing the lightning and EMP susceptibility of advanced electronic subsystems. The ALOFT NWDS, which consists of a central Navigation and Weapons Delivery

---

[1] Walko, L.C., "A Test Technique for Measurement of Lightning-Induced Voltages in Aircraft Electrical Circuitry." Technical Report NASA CR-2348, February 1974.

Computer (NWDC) and several peripheral units, has been modified to permit operation of the system in either the conventional hard-wire configuration or a fiber optics configuration, where the data cables are replaced by multiplexed fiber optics data links.[2] Although external adapter units were used to interface the existing peripherals to the fiber optics, the NWDC itself was extensively redesigned to accept the fiber optics through special connectors while maintaining the unit's shielding integrity.

This is important because the NWDC is therefore representative of a component that might be used in any other fiber optics system, and the change in susceptibility of this component to the lightning induced transients between the wire and the fiber optics configurations will show the advantage gained by use of fiber optics -- and this with general applicability to other systems, not just the A-7 ALOFT aircraft.

It should also be noted that the hard-wire signal cabling in the A-7 NWDS is exclusively double-shielded coax. Thus, even in the wire configuration, the A-7 NWDS would be considered a well designed and "hardened" system with respect to induced effects from lightning or EMP. This fact should be borne in mind when extending the results of this test to considerations of fiber optics performance against other types of wire configurations, such as twisted-pair unshielded or single-wire unshielded.

---

[2] Ellis, J.R., LCDR USN, "Interim Progress Summary and Description of A-7 ALOFT System." NELC Technical Report 1968 (TR 1968). Naval Electronics Laboratory Center, San Diego, California, January 1976.

1.3 Test Objectives

1.3.1 Primary. The primary objective of this simulated lightning test was to quantitatively determine the reduction in lightning transient susceptibility afforded by the use of fiber optics in the Navigation and Weapons Delivery Computer. Since the NWDC was substantially redesigned to accept the fiber optics while maintaining its shielding integrity, and is representative of a system that might be used in other aircraft applications, it was an excellent subsystem to demonstrate the advantage gained by the use of fiber optics.

1.3.2 Secondary. A second but also important objective of this test was to isolate and determine the relative importance of the induced transient components observed within the NWDC due to each of the three lightning coupling mechanisms: (1) Direct electromagnetic coupling into the NWDC, (2) Transients induced in the NWDC through the power wiring, and (3) Transients induced in the NWDC through the signal wiring.

2. TEST DESIGN

2.1 Approach

A 2000-ampere peak current pulse was applied to the aircraft to simulate the lightning current. This pulse was characterized by an approximate 1.6 microsecond risetime and 50 microsecond decay to half value. In order to allow a maximum of information to be drawn from the test, the NWDC was tested in a total of seven different configurations; these included variations in connections of the power cabling, signal cabling, fiber optics cables, and aircraft power.

Induced transient measurements were made on a total of 6 different circuits within the NWDC in each of the above configurations. Multiple observations of each transient were made (3 to 10) in order to allow confidence bounds on the data to be established. In addition to recording the time-domain transient waveforms, most waveforms were also analyzed with the Fast Fourier Transform to yield spectral information.

2.2 Lightning Simulation

2.2.1 Generator Configuration. A triggered capacitor bank, shown schematically in Figure 1, was used to produce the desired simulated lightning pulse.

The capacitor bank consisted of two sections of 4.8 μfd each. These were charged in parallel by a network of resistors, and discharged in series through a system of three spark gaps. During the test each section was charged to 31 kilovolts, which resulted in an output voltage of 62 kilovolts and an effective capacitance of 2.4 μfd.

Of the three spark gaps, only the center ball-gap was triggered. The others were adjusted to break down once the center gap had been closed. The center gap was "triggered" by a pneumatic cylinder which inserted a third ball within the gap, thus mechanically reducing the effective gap to nearly zero. This shifted the full potential of the charged bank to the two other gaps, causing them to break down immediately.

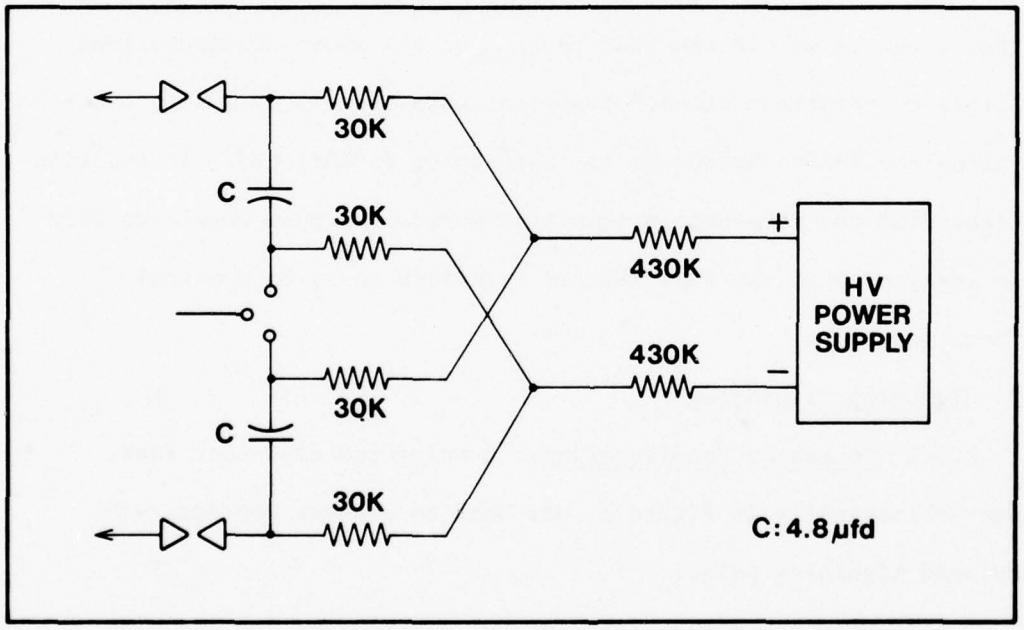

FIGURE 1. Pulse Generator Configuration

The two untriggered gaps were connected to the aircraft circuit through waveshaping resistors (not shown). These were required to insure that the discharge circuit was overdamped overall (to prevent oscillation of the output current), and to allow control of the pulse risetime. For this test, 15 ohms resistance was connected in each leg of the circuit resulting in a total of 30 ohms resistance added to the generator discharge circuit.

2.2.2 Applied Current Waveform. The applied current waveform used throughout this test was a double exponential pulse with 1.6 microsecond risetime and 50 microsecond decay time to half value. The peak current of this pulse was 2000 ($\pm$ 100) amperes. Figures 2 and 3 show the computer displays of the applied current pulse waveform, but first a brief explanation on interpretation of the computer displays which will be used throughout this report.

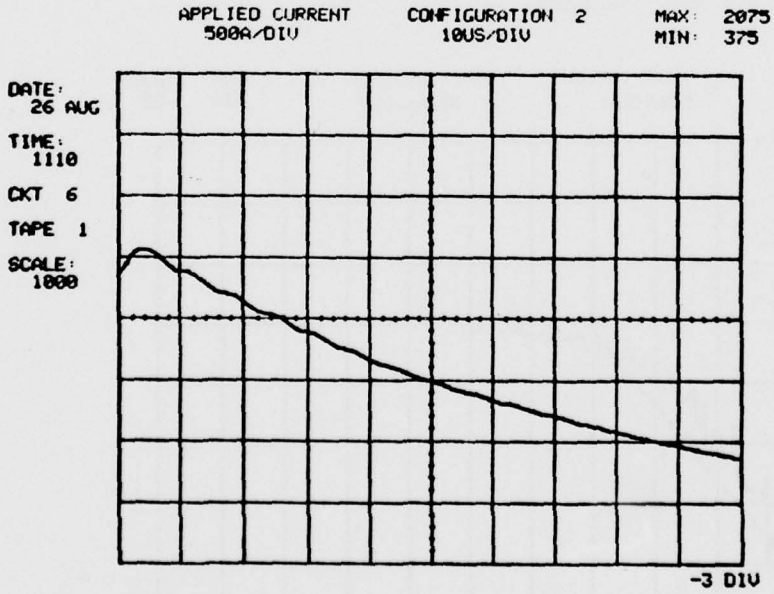

FIGURE 2. Applied Current Pulse - Overall

The graticule of the displays can be interpreted like that of an oscilloscope. The zero reference for each graph, however, may change from one display to the next; the number appearing at the lower right corner of the graticule indicates the position of the zero reference for each display. This number always represents the zero position with respect to the center of the graticule; thus, "-3 DIV" indicates that the zero reference is one division from the bottom of the graticule or 3 divisions below the graticule center. At the top of the graticule the vertical and horizontal scale factors are displayed, "500A/DIV" and "10 μS/DIV", respectively, the MAX and MIN information printed at the extreme upper right of the display represents the largest and smallest values of the waveform being displayed. The remainder of the information displayed around the periphery of the graticule is information used to record and identify each of the hundreds of waveforms recorded during the test.

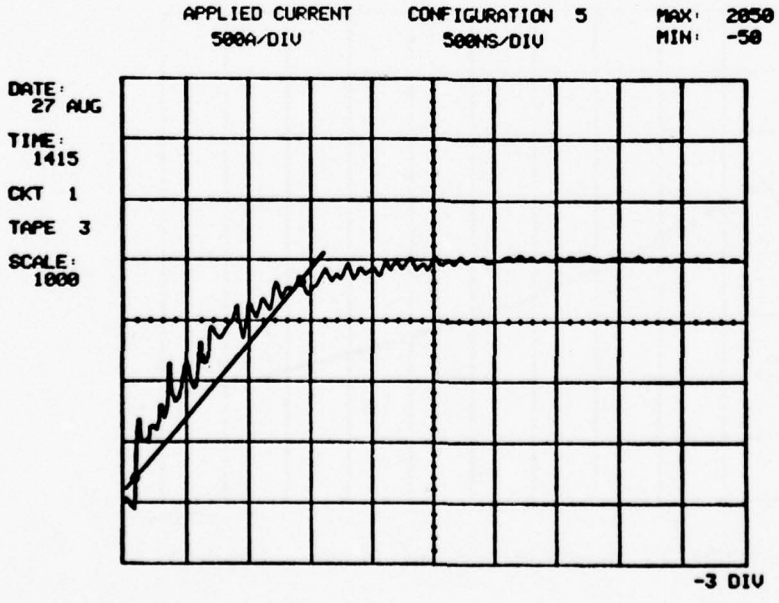

FIGURE 3. Applied Current Pulse - Leading Edge

Figure 2, at the relatively slow sweep speed of 10 microseconds per division, shows that the decay time to half value of the test waveform was about 50 microseconds, and that the peak value was 2075 amperes. At this sweep speed the instrumentation was unable to resolve the leading edge of the pulse, so that information must be obtained from a measurement at a faster sweep. This was done with the measurement shown in Figure 3, which shows that the peak value of the waveform occurred after about 5 microseconds, and that the peak current was 2050 amperes. The risetime of this waveform, defined by the extrapolation of the 10%-90% points on the leading edge of the pulse up to the peak value, was 1.6 microseconds.

The RF noise on the leading edge of the pulse, visible in Figure 3, was determined during the test to be stray pickup by the coaxial cable connected to the current transformer used to measure the applied pulse. This apparent noise was greatly reduced by added shielding along the length of cable, but the amount visible was the residual which could not be eliminated from the measurement system. This noise is considered to be an artifact of the measuring system and not a component of the applied current.

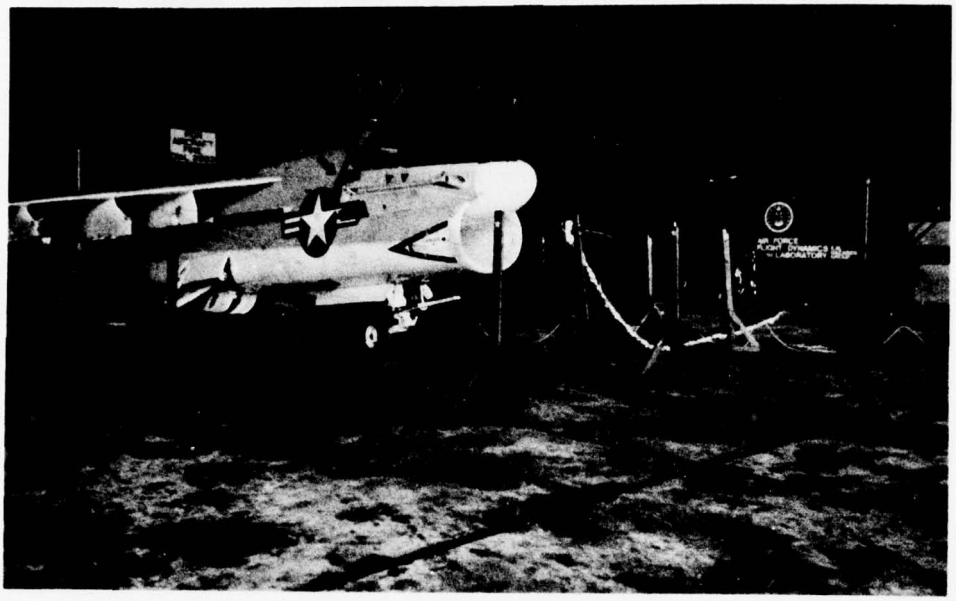

FIGURE 4. Overall Test Configuration

2.3 Equipment Configuration

2.3.1 Overall. Figure 4 is a view of the overall test area, the aircraft, and the current return lines, with the instrumentation van in the background. The pulse generator was placed approximately 8 feet behind the tail of the aircraft, as shown in Figure 5. The current return path was formed by a system of 4 parallel wires (for reduced overall circuit inductance), in the form of a large elliptical loop. The full pulse current passed through the aircraft, and the current was then divided approximately equally in half and returned to the generator via the two halves of the loop. The minor axis of this loop was 46 feet while the major axis was 56 feet.

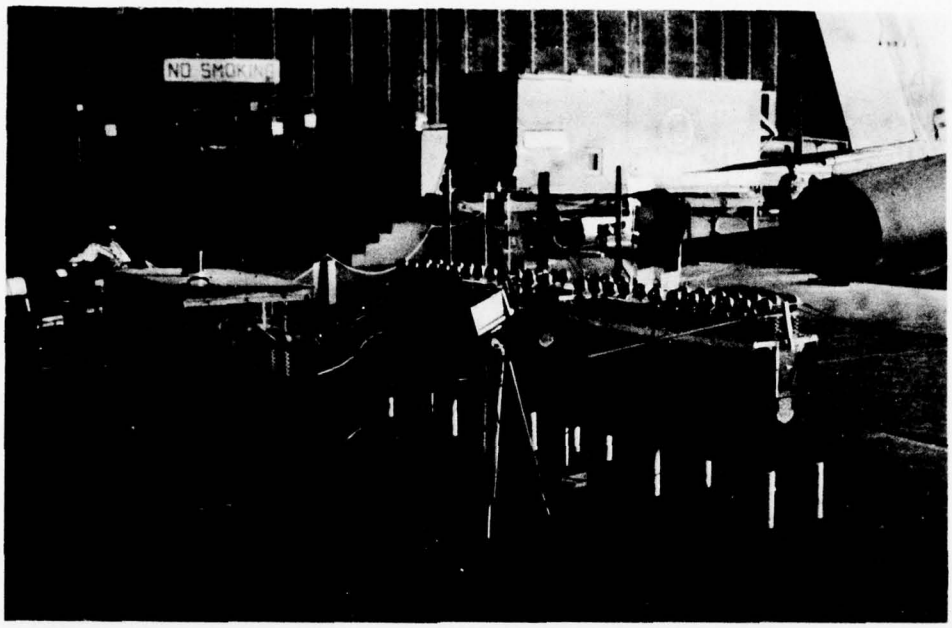

FIGURE 5. Pulse Generator Installation

Figures 6 and 7 show the method of attachment of the current return wires to the aircraft nose and tail. In each case, a mechanically sound connection was made to a cleaned metallic portion of the aircraft structure. The tail attachment was made at the base of the ECM antenna, which required the addition of a styrofoam cup as insulation, to prevent inadvertent arcing to the sensitive antenna rather than direct connection to the structure.

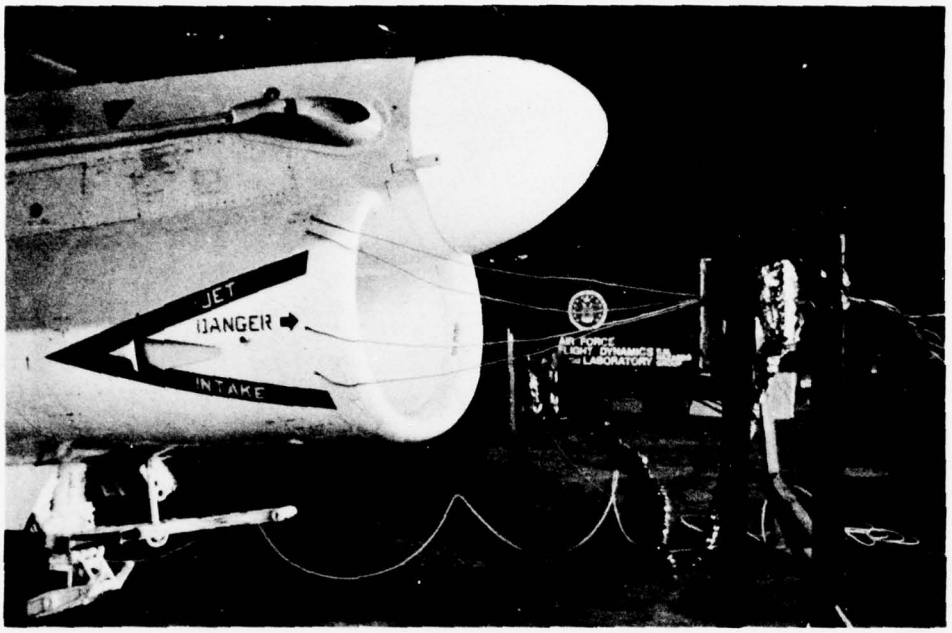

FIGURE 6. Pulse Generator Aircraft Nose Attachment

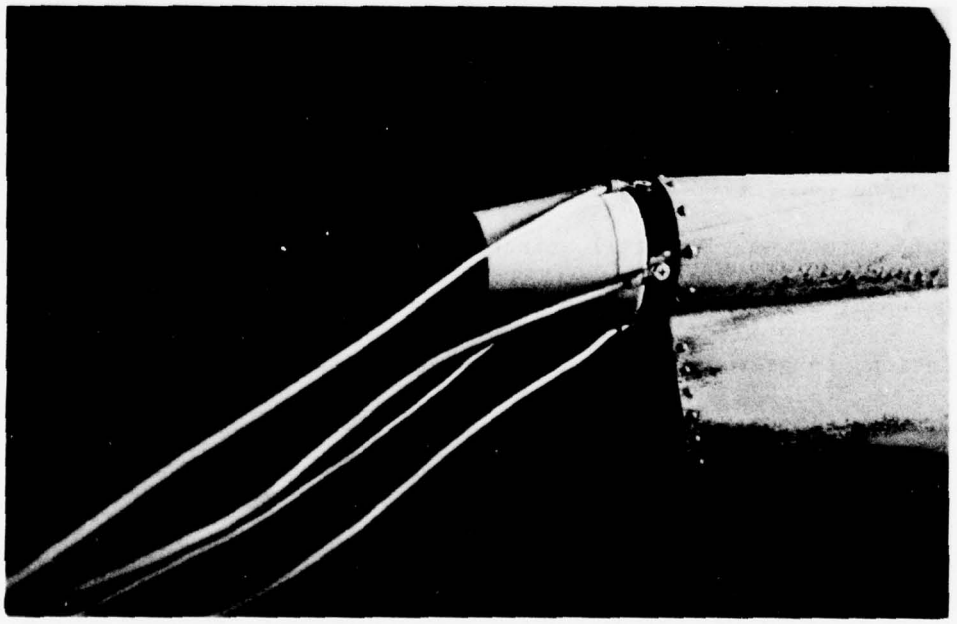

FIGURE 7. Pulse Generator Aircraft Tail Attachment

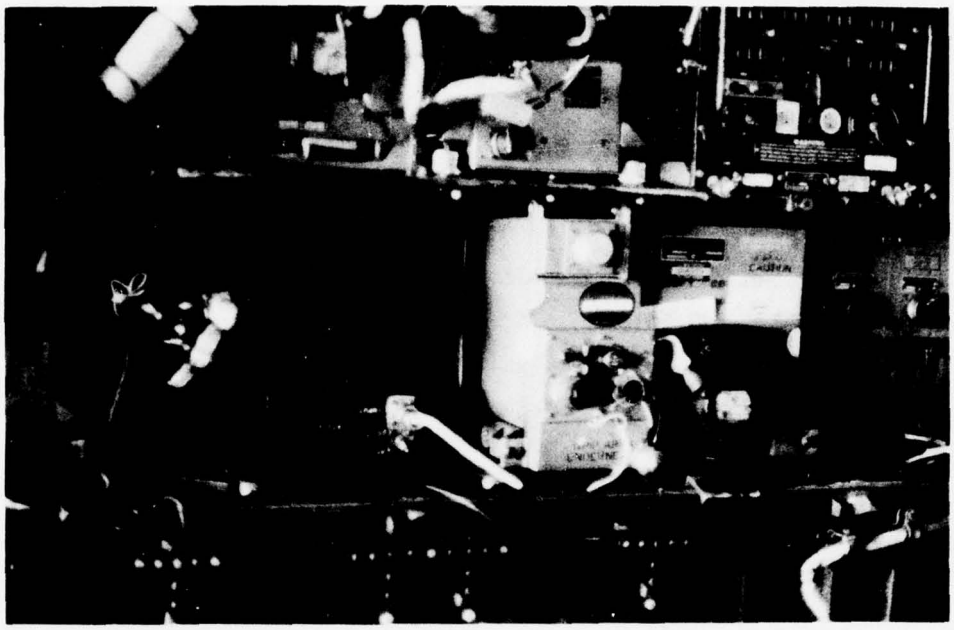

FIGURE 8. Fiber Optics Transmitter Installation

Figure 8 shows the installation of the fiber optics transmitter within the left hand equipment bay of the aircraft, where the NWDC was located. Connections to the induced circuits within the NWDC that were to be monitored were made via two 8-inch lengths of shielded wire.

As shown in Figure 9, all connections to the NWDC were made through J3, the AGE (Aerospace Ground Equipment) connector on the computer itself. The shielded wires from the measurement system fiber optics transmitter were terminated in pins to mate with J3. This allowed a simple and direct method of attachment.

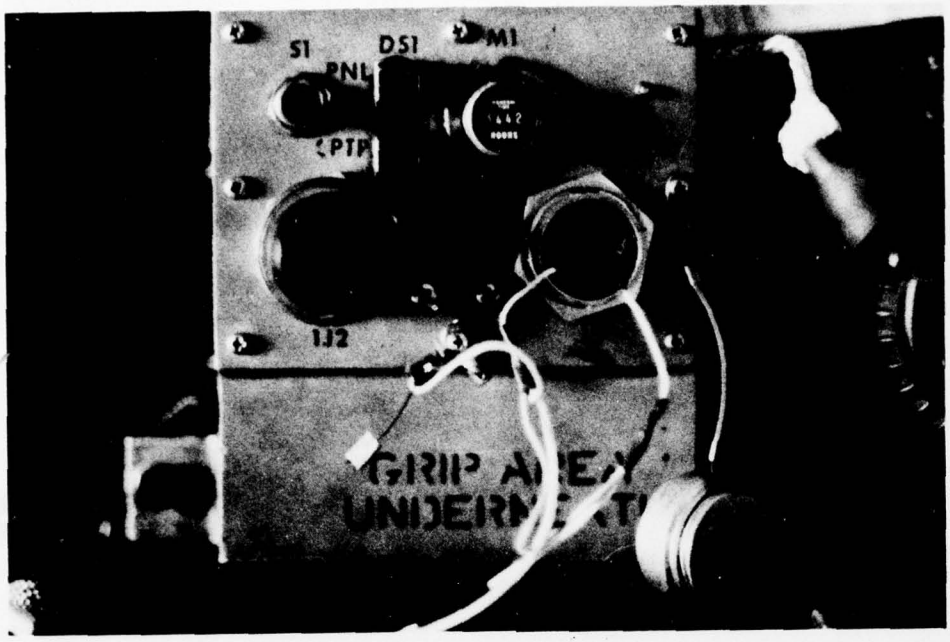

FIGURE 9. Induced Measurement Connection to NWDC

2.3.2 Aircraft. Prior to the start of testing, it was necessary to make the aircraft safe from any small air arcs that might occur across structural joints due to the high current which would be passing through the fuselage. All explosives associated with the ejection seat and canopy were removed. The aircraft fuel system was inerted by the following procedure: (1) The initial partial fuel load of JP-4 and JP-5 was drained, (2) the aircraft was filled with JP-5, and again drained, (3) a flow of nitrogen was maintained through the now empty fuel system for a period of 2 hours, and (4) the fuel system was filled with JP-5. Nitrogen flow through the system was started 1 hour before the start of testing each day, and maintained until the end of testing.

Throughout the test, the aircraft was securely grounded by a 5-foot-long cable to a point within the nose gear well. All equipment

bay doors remained closed throughout testing, and the aircraft wings were in the in-flight position. The canopy remained open.

2.4 NWDC Configurations

Table I, below, lists the seven configurations in which the Navigations and Weapons Delivery Computer was tested. The induced measurements made while the system was in Configuration 2 indicate the signals due solely to coupling directly into the computer itself, since no other wires were connected. Measurements made in Configuration 2 represent the response of the system in the full fiber optics configuration (but with aircraft power off). It was desired to make a series of measurements with the system in the fiber optics configuration and with power on, but this was not possible without connecting several of the hard-wire connectors to the computer also. For this reason, no measurements were made in this configuration.

TABLE I. NWDC Configurations

Configuration	Power Cabling	Hard Wire Signal Cabling	Fiber Optics Cabling	Aircraft Power
2	Off	Off	On	Off
3	On	Off	On	Off
4	On	On	Off	Off
5	On	Off	Off	Off
6	On	On	Off	On
7	Off	On	Off	Off
8	Off	Off	Off	Off

Configurations 4 through 8 were with the NWDC in the wire configuration. Configuration 4 measurements are indicative of the system performance with all necessary cabling in place, but with power off. Comparison between configurations 3 and 4, therefore, shows the advantage gained by the use of fiber optics in this system. Configuration 5 measurements indicate the transient response of the system with only the power cabling connected, while measurements made while the system was in Configuration 6 represent responses in the complete hard-wire configuration with power on. Configuration 7 isolates the transient components due to the hard-wire signal cabling, while Configuration 8 measurements show the response of the NWDC itself to the field environment when it was in the wire configuration internally.

While Configurations 3 and 4 form the comparison for the hard-wire versus the fiber optics configuration, the other configurations allow further conclusions to be drawn regarding the relative amounts of transient energy being coupled into the system by the various wiring systems. Comparisons of the results of the measurements in Configuration 6 with those obtained in Configuration 4 will allow some extrapolation of the results of all other configurations to what might be expected were the system in operation with power on.

2.5 NWDC Circuits of Interest

Six circuits within the NWDC were chosen to be monitored in each of the seven system configurations. These were chosen to show the changes that occurred in the data sections of the computer, the electro-optical interface sections, and the power supply. Each of

the circuits was assigned a number to allow identification of each recorded waveform with the circuit being monitored.

2.5.1 NAV Panel Data Out. Circuit #1 was the signal identified within the NWDC as "NAV Panel Data Out." This is a data output signal from the computer to the peripheral. As shown in Figures 10 and 11, this signal was accessed through pins 82 and 91 of the NWDC AGE connector, J3. This signal represented one side of a differential

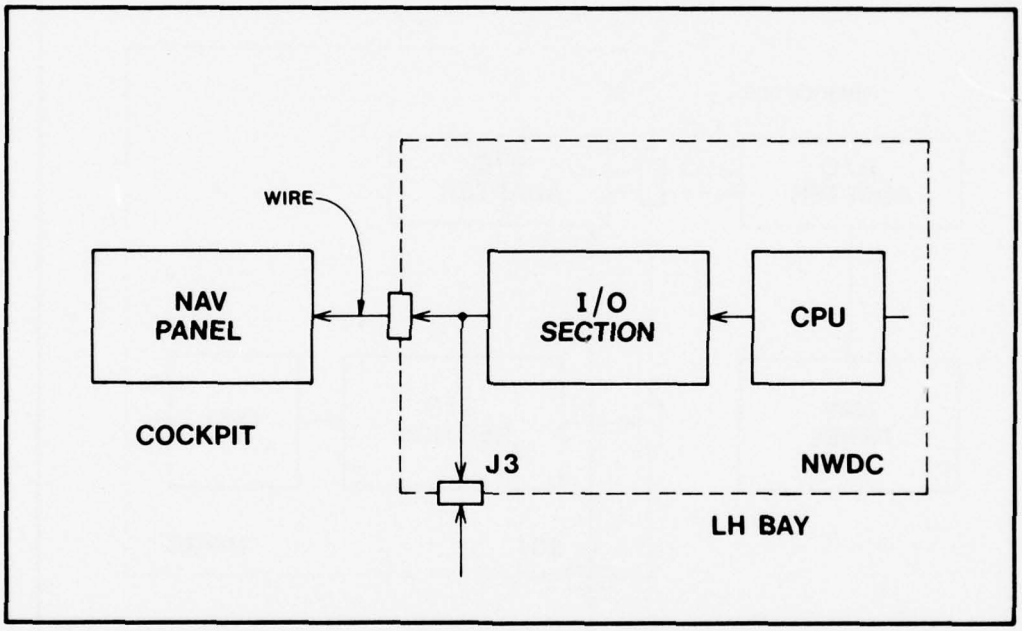

FIGURE 10. Circuit 1 with NWDC in Wire Mode

circuit, and was common to both the fiber optics and hard-wire configurations. Thus changes in signal level at this point between the fiber optics and wire modes show the effects of the differences in transient coupling between the two configurations. The NAV Panel is located in the cockpit area, and the length of the cable run (wire or fiber optics) between it and the NWDC is approximately 30 feet.

2.5.2 Data Output to FLR Signal Generator. Circuit #2 was the signal identified within the NWDC as "Data Output to FLR (Forward Looking Radar) Signal Generator." This is a data output signal from the computer to the peripheral, and was accessed through pins 83 and 91 of NWDC connector J3. Figures 10 and 11 are also descriptive of the measurement point in this circuit, except that the peripheral box in the diagram should read "FLR Signal Generator" rather than

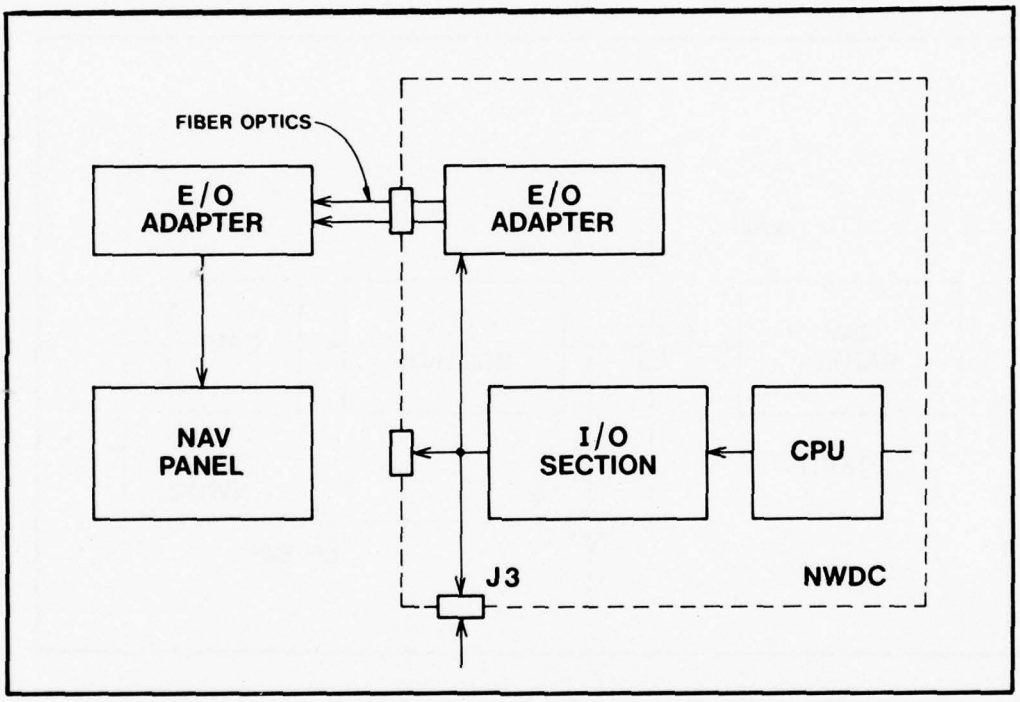

FIGURE 11. Circuit 1 with NWDC in Fiber Optics Mode

"NAV Panel." This measurement point is again common to both the wire and fiber optics configurations. The FLR Signal Generator is located in the mid equipment bay, and the length of the cable run between it and the NWDC is approximately 20 feet.

2.5.3 HUD Data Out (True). Circuit #3 was the signal identified as "HUD Data Out (True)." This is a data output signal from the computer to the peripheral, and was accessed through pins 84 and 91 of NWDC connector J3. Figures 10 and 11 are again descriptive of this circuit if the HUD (Heads Up Display) is substituted for the NAV Panel in the diagram. The HUD is located in the left hand equipment bay, as is the NWDC, so the cable length is only about 5 feet. This measurement point was also common to both the wire and fiber optics configurations.

2.5.4 NAV Panel Receiver Output. Circuit #4 was the output of the fiber optics receiver operational amplifier, as shown in Figure 12. This point was within one of the E/O (electro-optical) adapter cards within the NWDC, and therefore was only monitored when the system was in the fiber optics configurations (2 and 3). This circuit was chosen to show the transient levels experienced by these new components within the computer. This circuit was accessed through pins 80 and 91 of connector J3.

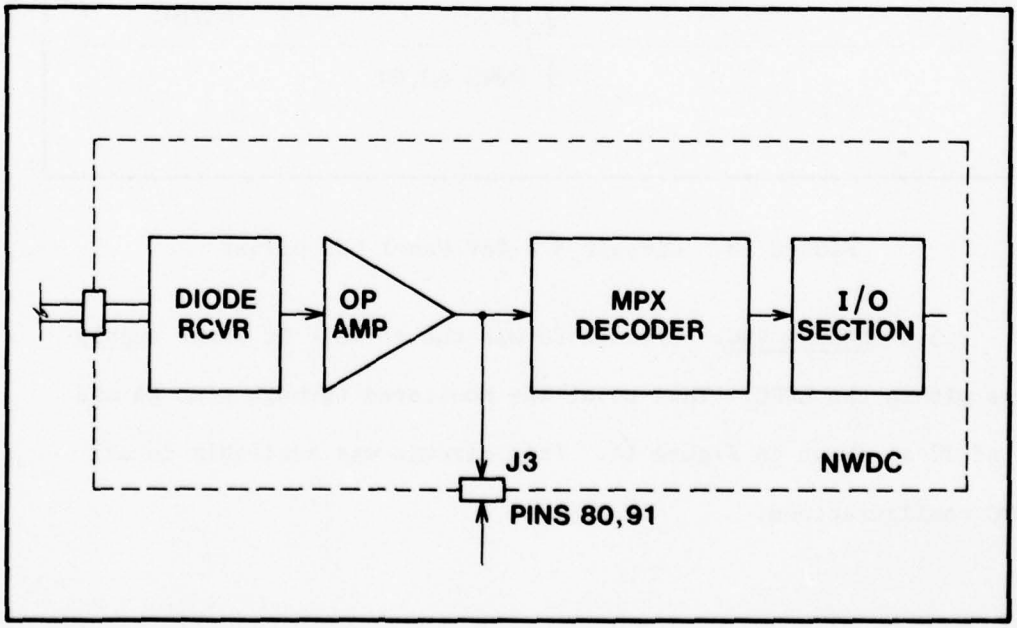

FIGURE 12. Circuit 4 - NAV Panel Receiver Output

2.5.5 NAV Panel LED Driver. Circuit #5 was the input to the logic gate driving the LED transmitter for the fiber optics link to the NAV Panel. As shown in Figure 13, this point in the E/O adapter circuit was monitored through pins 48 and 91 of J3. This circuit was also only available for monitoring when the computer was in the fiber optics configurations.

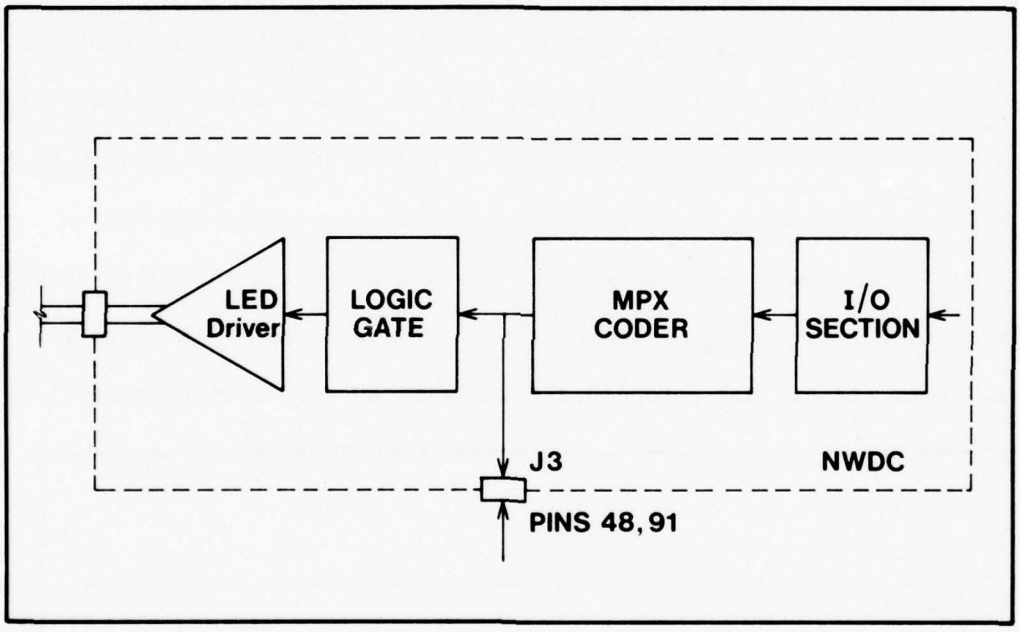

FIGURE 13. Circuit 5 - NAV Panel LED Driver

2.5.6 NWDC + VDC. Circuit #6 was the +5 volt DC power supply line within the NWDC. This point was monitored through pins 85 and 91 of J3 as shown in Figure 14. This circuit was available in all NWDC configurations.

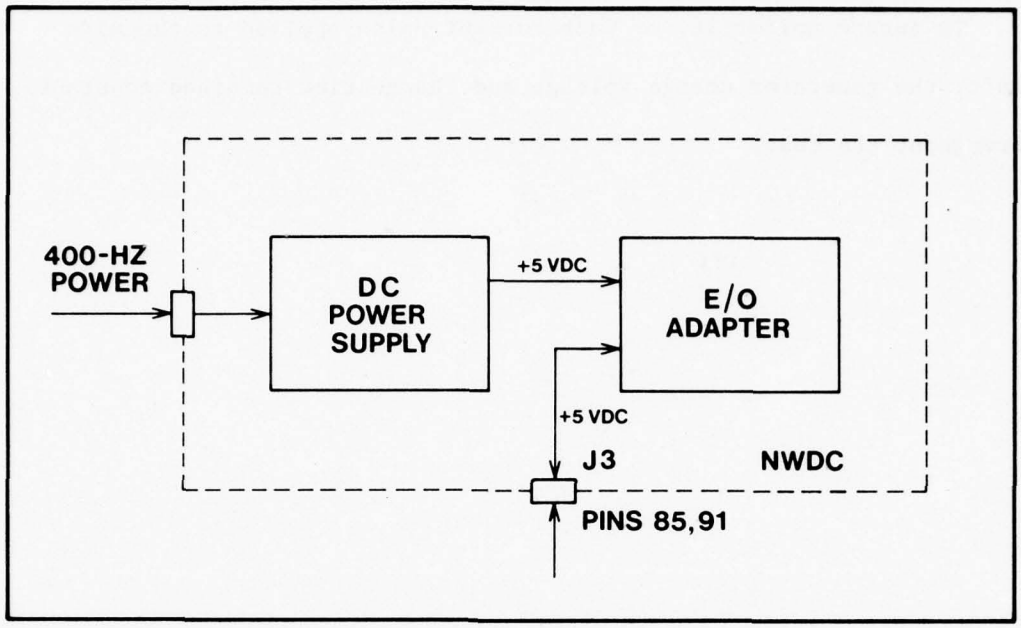

FIGURE 14. Circuit 6 - NWDC +5 VDC

2.6 Procedure

Before the start of each day's testing, nitrogen was passed through the aircraft fuel system and the vapors being vented were checked with an explosimeter. The measurement fiber optics system was then installed and connected to the first circuit to be monitored that day. The lightning simulation generator was then fired at 1 minute intervals until all measurements on that circuit had been completed. The generator was then discharged and made safe by shorting cables so that the connections to the fiber optics measuring system could be changed to the next circuit to be monitored.

This process was repeated until it became necessary to change the NWDS configuration and begin a new measurement series.

To insure uniformity of each current pulse applied to the aircraft, the generator change voltage and charge time remained constant throughout the test.

3. INSTRUMENTATION

3.1 Waveform Digitizing Instrumentation

3.1.1 Overall. A Tektronix WP 2221 Waveform Digitizing Instrumentation package was used during this test to perform and record all transient measurements. This system is pictured in Figure 15, and consists of an R7912 Transient Digitizer, PDP-11/05 minicomputer, magnetic tape drive, graphics terminal, and a printer.

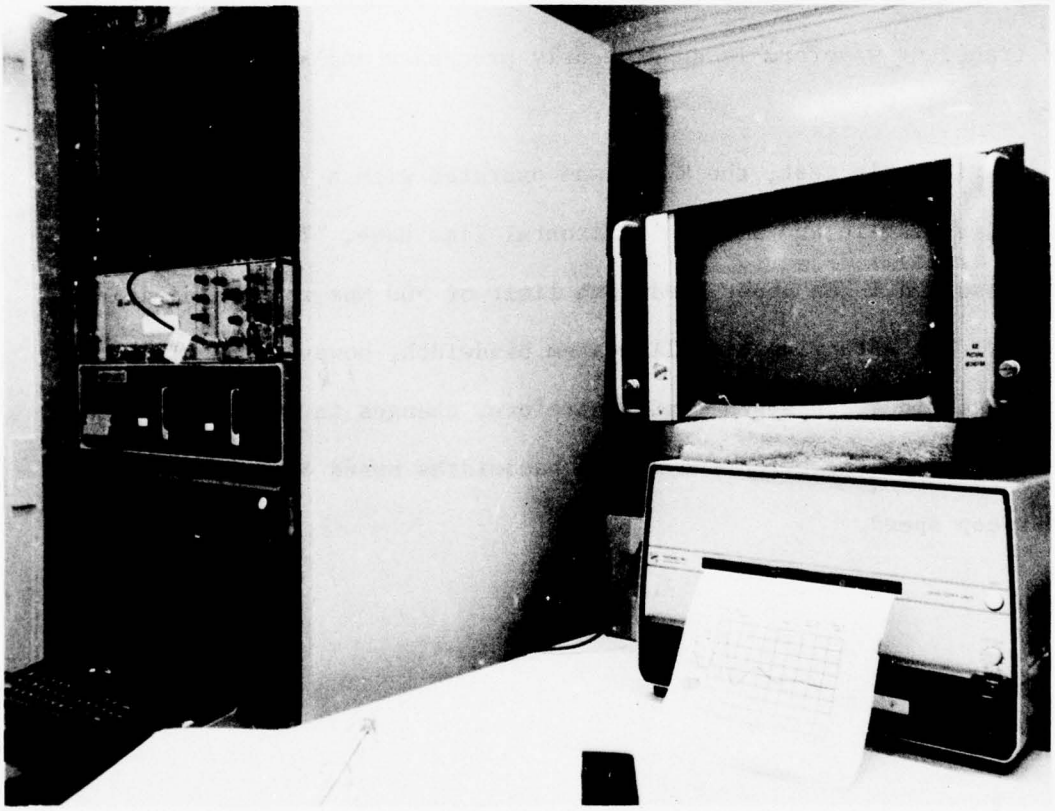

FIGURE 15. Waveform Digitizing System

3.1.2 R7912 Transient Digitizer. The Tektronix R7912 Transient Digitizer is a high-speed analog-to-digital converter which can sample at rates up to 1 GHz. It has the capability of storing raw data in an array of up to 4096 9-bit digital words with a resolution sufficient to discern 512 distinct vertical levels in each sample.

The R7912 is operated much like an oscilloscope, with the exception that its output can either be viewed on a TV monitor or diverted directly to the minicomputer. For handling by the minicomputer, the raw data array is reduced to an array of 512 elements or samples. The transient waveform is subsequently processed and stored in this form.

During this test, the R7912 was operated with a 7A19 Vertical Amplifier plug-in and a 7B92A Horizontal Time Base. This configuration resulted in an upper bandwidth limit of 500 MHz for the digitizer system. The effective overall system bandwidth, however, is affected by changes in sweep speed (and, therefore, changes in sample rate). Table II shows the effective system bandwidths based on sample period and sweep speed.

TABLE II. R7912 Effective System Bandwidth

SWEEP SPEED (PER DIVISION)	TIME WINDOW WIDTH	SAMPLE PERIOD (51 SAMPLES/DIV)	EFFECTIVE* DIGITIZER SYSTEM BANDWIDTH
100 nS	1 US	2 nS	250 MHz
500 nS	5 US	10 nS	50 MHz
1 US	10 US	20 nS	25 MHz
10 US	100 US	196 nS	2.5 MHz

* Based on Nyquist frequency.

nS = nanoseconds

US = microseconds

(Note that these bandwidth figures apply to the digitizer system only. Since all measurements were made via the fiber optics measurement system (para 3.2), the upper frequency limit was 25 MHz.)

3.1.3 Minicomputer. The PDP-11/05 computer forms the hub of the Waveform Digitizing Instrumentation and makes possible the operation of the various devices as an instrumentation system. When not being used to control the Transient Digitizer, the computer can also be used (with its BASIC language interpreter) to perform normal computational tasks.

The system operates under control of WDI TEK BASIC, a Tektronix software package. All communications with the digitizing hardware is accomplished within this software, in addition to normal programming. The software has essentially all the capabilities of BASIC language interpreters for other computer systems, with the addition of several very powerful commands of specific value in waveform processing.

3.1.4 Peripherals. Input/output for the digitizing system is handled by three units. Real-time operator communication with the system is accomplished with a Tektronix 4010-1 Graphics Terminal having alphanumeric and graphics capability, while the Tektronix 4610 Hard Copy Unit can provide permanent paper copies of information displayed at the terminal. The CP100 dual cassette drive provides a means of storage and retrieval of programs, data files, and waveform files using magnetic tape cassettes.

3.1.5 System Operation. Figure 16, below, represents schematically the operation of the individual units comprising the digitizing instrumentation. During this test, all induced transient measurements were made with a fiber optics analog data link system to couple the R7912 to the circuit within the aircraft that was being monitored.

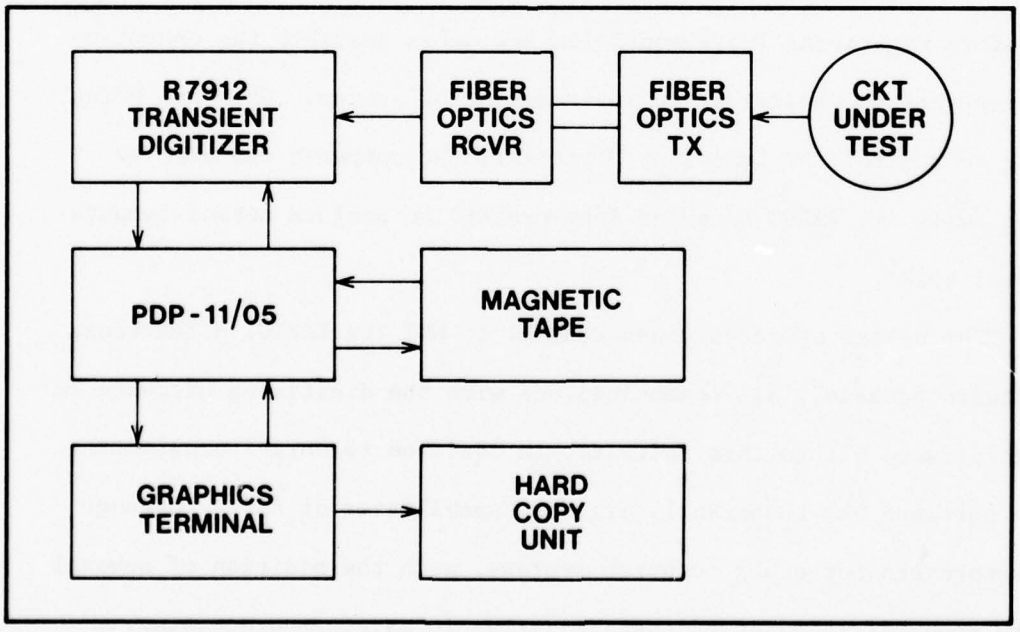

FIGURE 16. Digitizing System Configuration

Under control from the computer, then, measurement information was displayed, analyzed, printed and stored in real time, reducing the requirements for later data processing on the stored waveform data.

3.1.6 ALOFT Test Software. For efficient utilization of the digitizing system, additional BASIC software was developed specifically for this test program. This software allowed rapid control of the Transient Digitizer and tape drives, while also enhancing real-time data displays and analysis. Using this software, one induced transient measurement (including digitizing, some analysis, display, printing and storage on tape) could be made every 45 seconds. A listing of the BASIC language program can be found in Appendix A.

3.2 Fiber Optics Measurement System

3.2.1 Description. A fiber optics measurement system was used for connecting the Transient Digitizer system to the circuits within the NWDC that were to be monitored. This practice reduced noise pickup (compared to coaxial cables as is usual practice), and also eliminated the need for establishing a common electrical ground between the aircraft and the instrumentation van. This system was built especially for this application, and as such, the electro-optical transmitter is housed in an RF-tight box with its rechargeable battery mounted internally. The transmitter box was placed within the equipment bay housing the NWDC itself, while the fiber optics cable connected the transmitter to its receiver system within the instrumentation van.

Figure 17, shows the general design of the system. It is built around the MDL 238 analog fiber optics system manufactured by Meret,

Inc.[3], with additional elements required for this application. The MDL 238 transmitter requires a 12 volt power source (200ma current draw), has a 75-ohm input impedance, and is limited to ± 0.5 volt input voltage. To use this unit in this application, it was necessary to add a step attenuator so that voltages of up to 40 volts peak could be measured. Since it is occasionally desired to monitor circuits with DC power applied to them, a provision was added for coupling the system to the circuit to be measured through two DC blocking capacitors (2 μF each) so that no overloading of the circuit under test, and no damage to the fiber optics system, would result. During this test the input impedance into the step attenuator was 50 ohms, and the DC blocking capacitors were not used in any of the measurements.

Twenty meters of optical fiber cable is used to connect the transmitter to its receiver system within the van. The MDL 238 receiver requires supply voltages of 6 and 30 volts, and produces a maximum output voltage of approximately 30 mV into a 500-ohm load. This load requirement and output voltage were unacceptable, so the addition of a wideband amplifier stage was required to increase the output signal level to 300 mV (peak) while allowing operation into a 50-ohm load (the 7A19 amplifier of the R7912). This added amplifier was a Hewlett-Packard type 641A.

---

[3]Meret, Inc., 1815 24th Street, Santa Monica, CA 90404

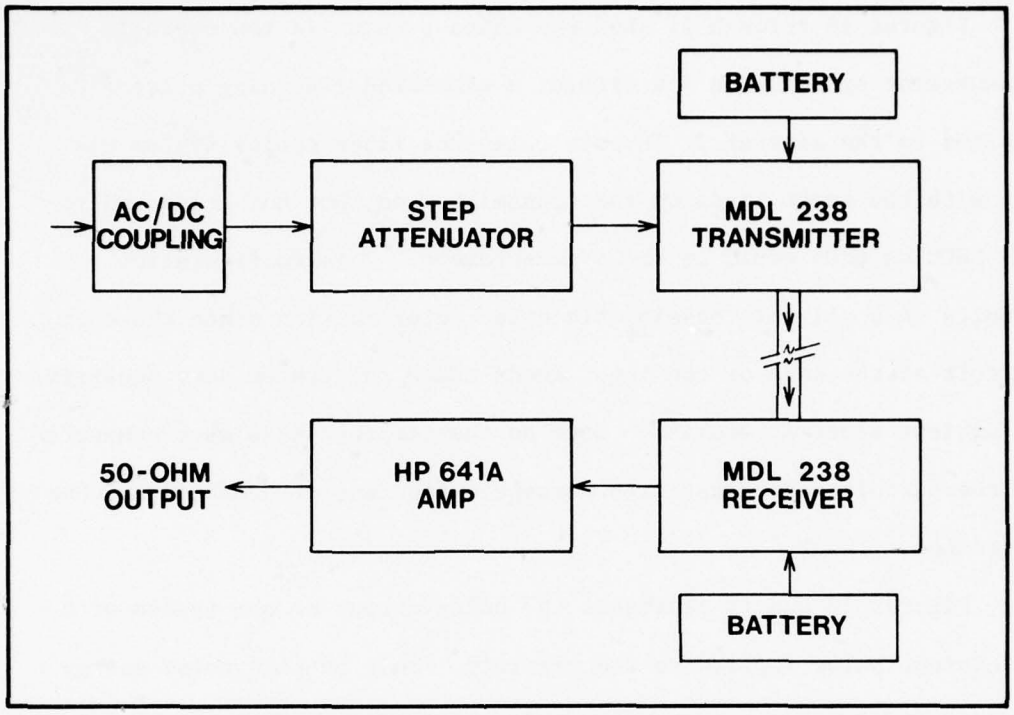

FIGURE 17. Fiber Optics Measurement System

3.2.2 Performance. This system responded to signals between 100 Hz and 50 MHz, though the gain of the system was approximately constant between 1 KHz and 25 MHz (the 3-dB points). The system would operate for over four hours with less than a 10% change in gain due to discharge of the transmitter batteries. The maximum output voltage of the system (into 50 ohms) was $\pm$ 300mV, while the maximum input voltage the modified transmitter could measure (with maximum attenuation) was 25 volts. Noise produced by the fiber optics unit itself was far below the inherent noise of the final wideband amplifier.

3.3 System Noise

Figures 18 through 21 show the noise present in the overall measurement system with and without a simulated lightning pulse applied to the aircraft. In both cases the fiber optics system was on, with the input leads to the transmitter on, but not connected to the NWDC as they would be for a measurement. This configuration results in a slightly pessimistic noise determination since the open circuit at the ends of the input leads makes the system very sensitive to ambient electric fields -- more so than if the leads were connected to the circuit under test with perhaps a few tens or hundreds of ohms impedance.

Figures 18 and 19 represent the noise output of the system with no current pulse applied to the aircraft. Most of this noise energy is directly from the wideband amplifier itself. The time domain plot

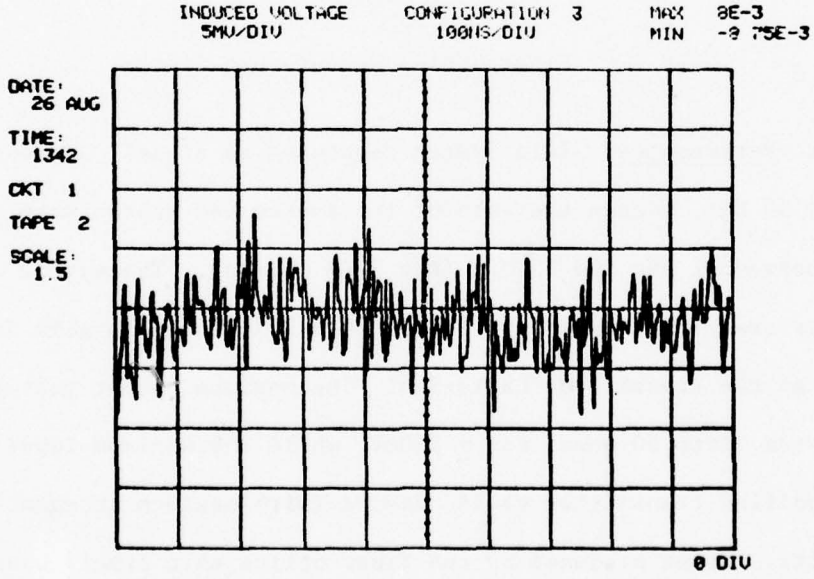

FIGURE 18. Measurement System Noise - No Lightning Pulse

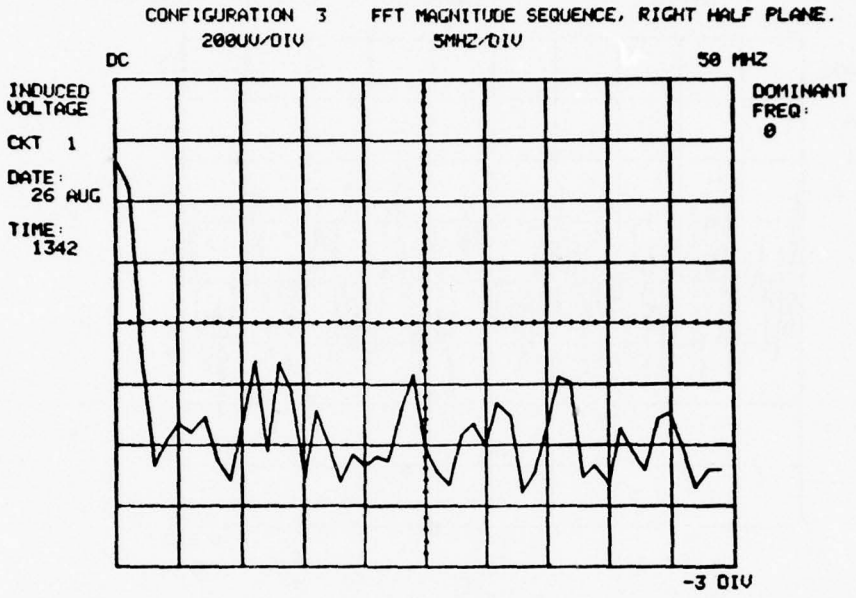

FIGURE 19. Frequency Spectrum of System Noise - No Pulse

shows the noise peaks to be +8 and -9 millivolts. The Fourier Transform spectrum shows a fairly even distribution of energy over the spectrum at very low magnitude. (In this plot zero frequency is displayed at the left of the graticule, with maximum frequency displayed at the extreme right.) The large apparent DC component was due to slight misadjustment of the recording equipment and is not of significance in this measurement.

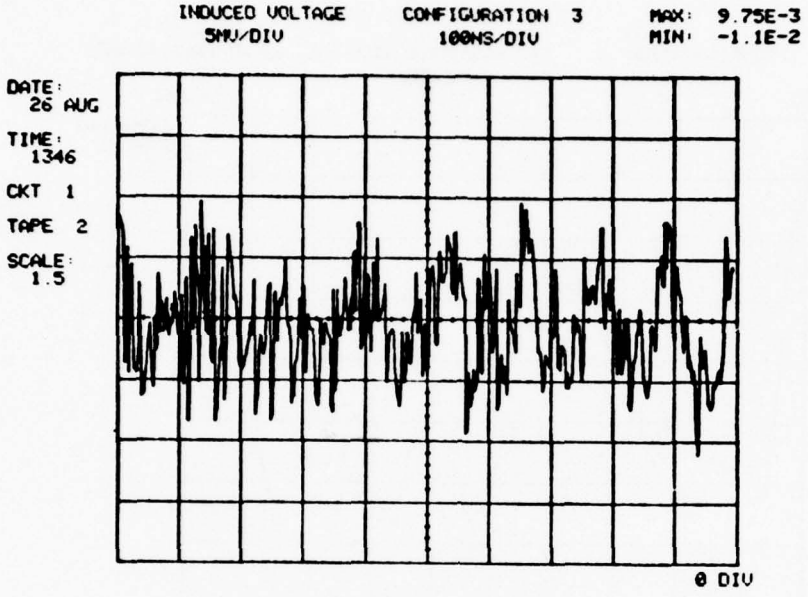

FIGURE 20. Measurement System Noise - With Lightning Pulse

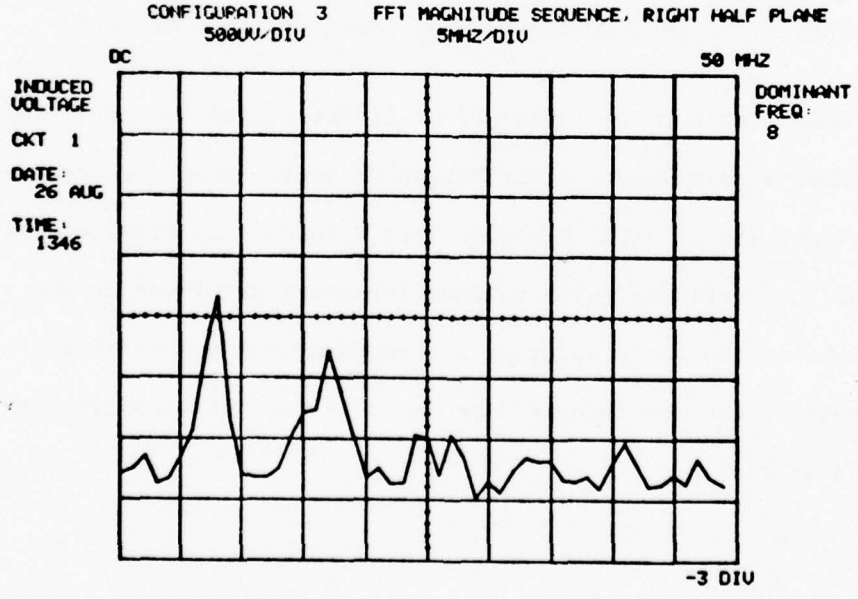

FIGURE 21. Frequency Spectrum of System Noise - With Pulse

Figures 20 and 21, on the other hand, show the noise output of the system with a pulse applied to the aircraft. This signal, though little higher in amplitude (+10 and -11 mV) contains relatively large amounts of energy at approximately 8 and 17 MHz. It was determined during the test that this characteristic spectrum was again a direct result of the wideband amplifier. It appeared to be due to energy coupling into the amplifier through the AC power line. The amplifier was not well shielded in this respect.

These waveforms are quite representative of the several noise measurements that were conducted throughout the test. The system noise level can then be considered to be about 10mV peak. It was also apparent that strong fields at approximately 8 and 17 MHz were present in the test area, since coupling through the power system was observed. (The instrumentation van housing the equipment was well shielded and grounded. The majority of stray pickup was due to the AC power system.)

3.4 Discrete Fourier Transform Notes

For those readers not familiar with the applications and limitations of the Discrete Fourier Transform (FFT), a good reference on digital signal processing or communication theory should be consulted to facilitate proper interpretation of the FFT displays in this report. Several other considerations are also applicable. First, the vertical scaling in the FFT displays is linear rather than logarithmic as is common. Second, only the positive half of the Fourier magnitude sequence is displayed, with DC displayed at the left margin of the

graticule and maximum frequency displayed at the right margin. Third, it is not, in general, possible to make comparisons of spectral energy content (area under the frequency spectrum curve) between different FFT displays due to the effects of leakage in the FFT computations and differences in time domain and frequency domain sample periods.

4. RESULTS

4.1 Fiber Optics Versus Hard-wire Comparison

In this section, the results obtained in NWDC configurations 3 and 4 will be compared. This effectively compares the transients between the fiber optics (#3) and hard-wire (#4) configurations. All measurements made in these configurations were with the system powered down.

4.1.1 NAV Panel Data Out (Circuit 1). Figures 22 and 23 show a typical transient waveform for Circuit 1 with the NWDC in the fiber optics configuration. This waveform is very similar to the system noise waveform, but about 3 times greater in amplitude. Most of the transient energy occurs around 8 MHz, which is also similar to the noise waveform. This similarity is to be expected since the only wires now connected to the NWDC are the power supply cables. Of the four repeat measurements made in this configuration the average peak amplitude of the signals were +26 and -26 millivolts.

Figure 24 and 25 show a typical transient for Circuit 1 with the NWDC in the wire configuration. The signal amplitude is now about 16 times greater than the noise, and it has a definite character different from the measured noise. Figure 25 shows that most of the energy in this transient occurs at 2.4 and 4.2 MHz, again quite different from the noise and the transient waveform observed in the fiber optics configuration. A total of eight repeat measurements were made, and the average peak voltages were +171 and -178 millivolts.

The transients on circuit #1 increased in magnitude by 550% in changing from the fiber optics to hard-wire configuration. In addition, the bulk of the energy in the transient shifted from 8 MHz to 2.4 and 4.2 MHz.

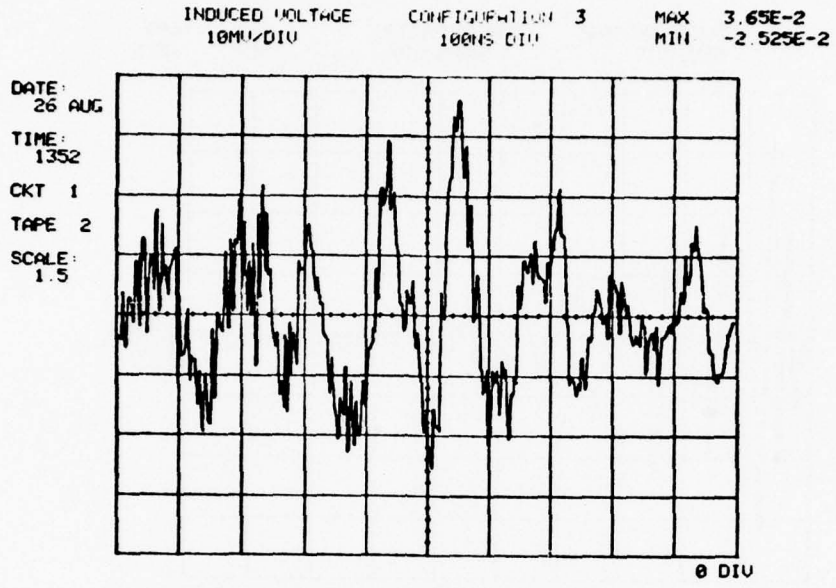

FIGURE 22. Induced Transient, Circuit 1, Fiber Optics Configuration (#3)

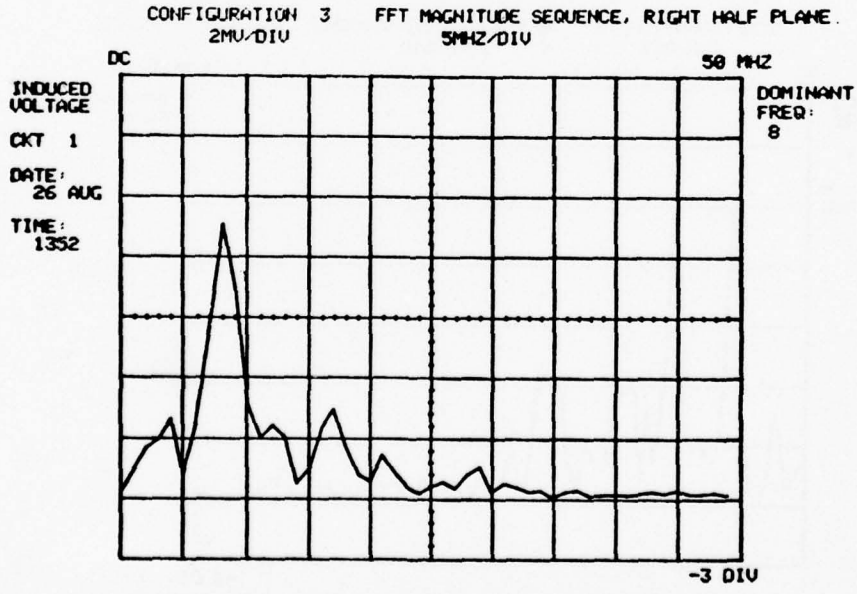

FIGURE 23. Frequency Spectrum, Circuit 1, Fiber Optics Configuration (#3)

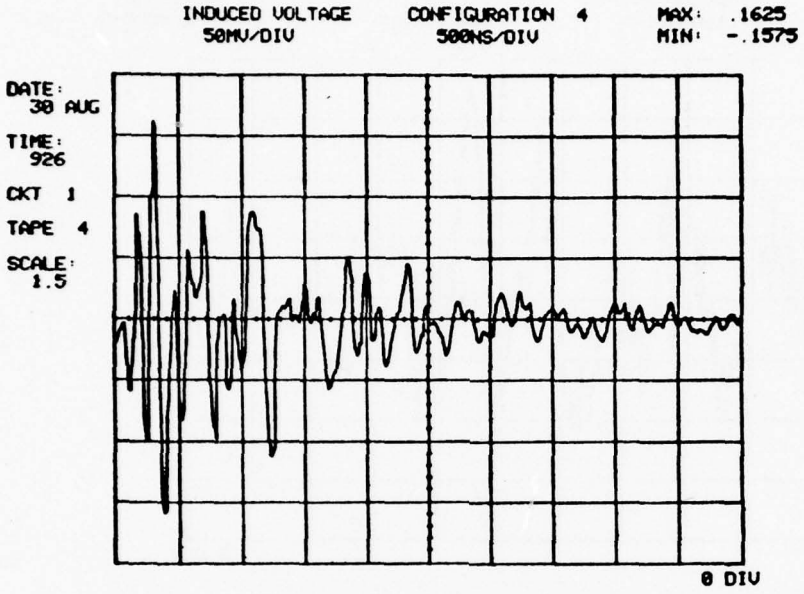

FIGURE 24. Induced Transient, Circuit 1, Wire Configuration (#4)

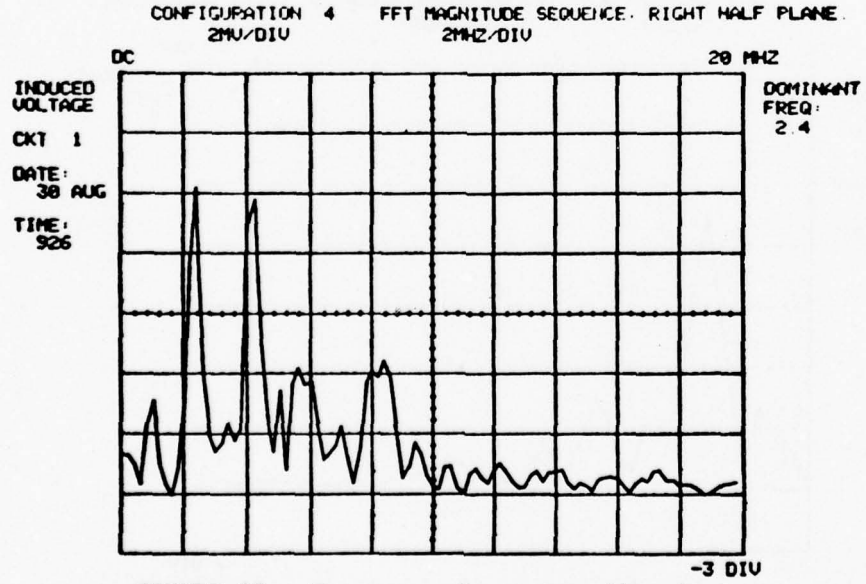

FIGURE 25. Frequency Spectrum, Circuit 1, Wire Configuration (#4)

4.1.2 FLR Data Out (Circuit 2). Figures 26 and 27 show a typical transient observed on Circuit 2 with the NWDC in the fiber optics configuration. Again, the waveform is very similar to the noise waveform but about 3 times greater in amplitude, as was the case with Circuit 1. Most of the transient energy is again concentrated around 8MHz as it was with the noise signal. Four repeat measurements were made of this waveform and the average peak values were +42 and -36 millivolts.

Figures 28 and 29 show the transient observed on this circuit with the NWDC in the wire configuration. Again, the character of this signal is very different from the noise. Its amplitude is 410 millivolts, which is 41 times greater than the observed noise. Most of the transient energy is now occurring at 900 KHz and 5.1 MHz. Eight repeat measurements were made on this waveform, and the average peak values were +382 and -336 millivolts.

The transients on Circuit 2 increased in magnitude by 810% in changing from the fiber optics to hard-wire configuration. In addition, the bulk of the transient energy shifted from 8 MHz to 900 KHz.

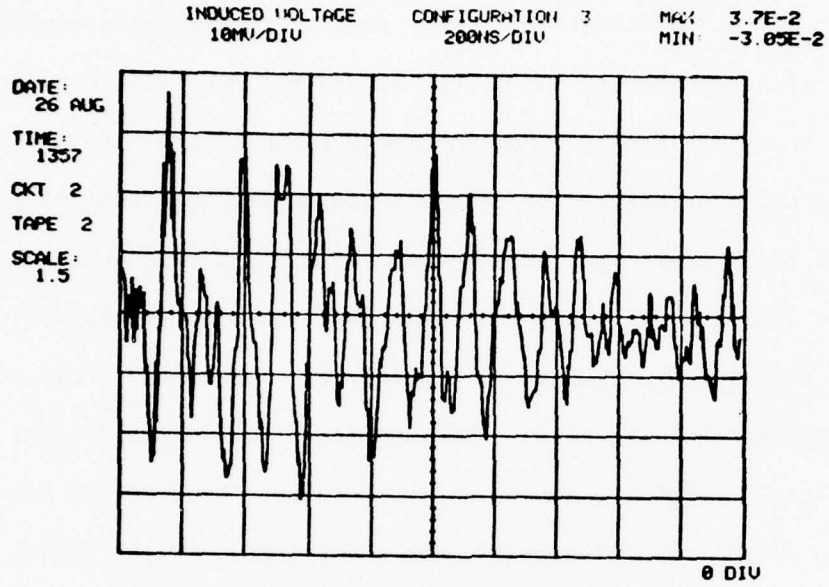

FIGURE 26. Induced Transient, Circuit 2, Fiber Optics Configuration (#3)

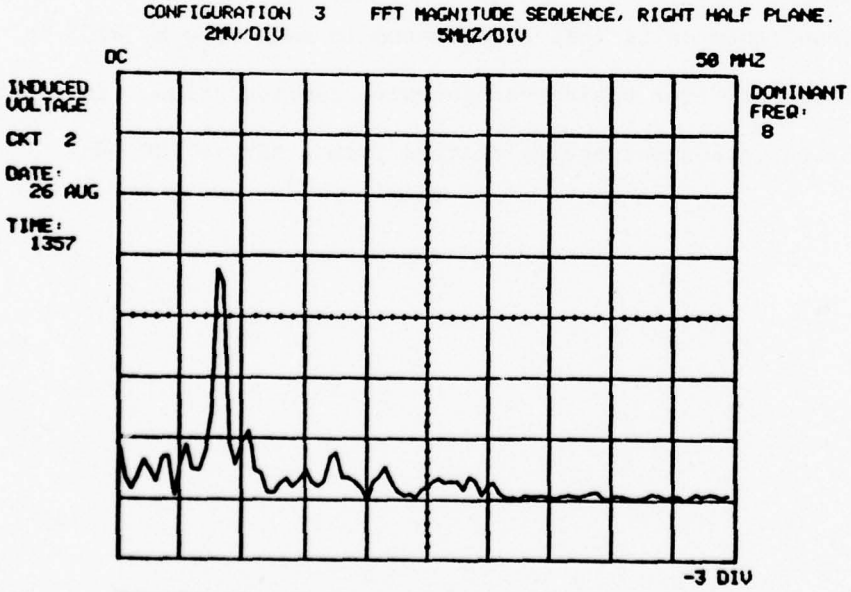

FIGURE 27. Frequency Spectrum, Circuit 2, Fiber Optics Configuration (#3)

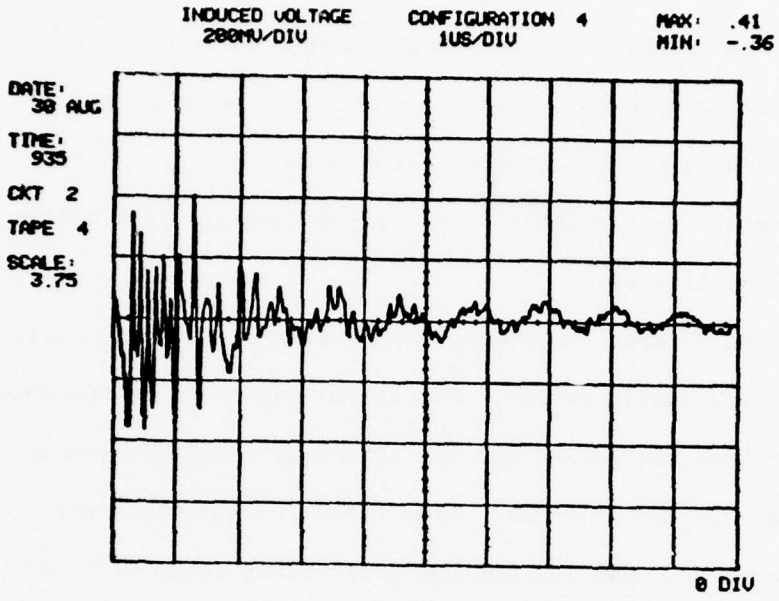

FIGURE 28. Induced Transient, Circuit 2, Wire Configuration (#4)

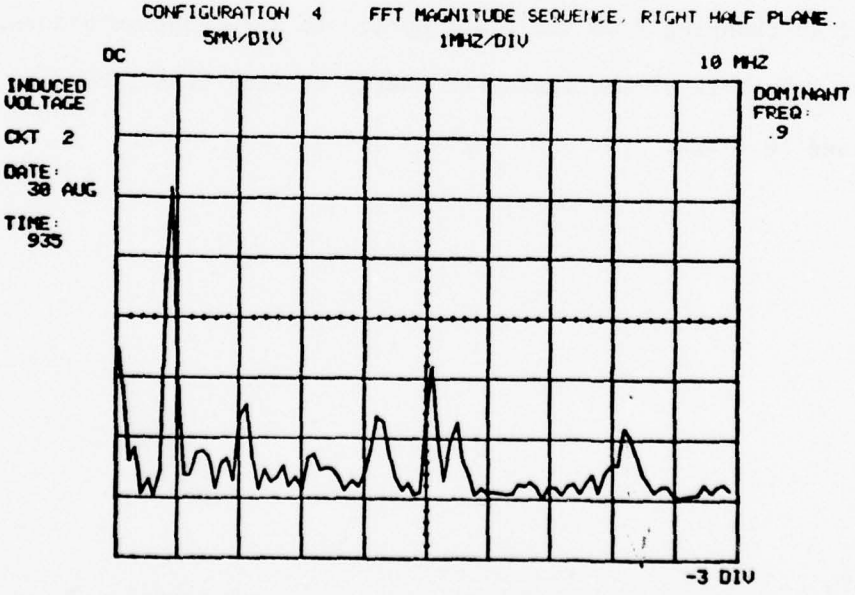

FIGURE 29. Frequency Spectrum, Circuit 2, Wire Configuration (#4)

4.1.3 HUD Data Out (Circuit 3). Figures 30 and 31 show a typical transient observed on Circuit 3 with the NWDC in the fiber optics configuration. Again, the waveform is not significantly different from the noise waveform, except that it is about twice as large in magnitude. The energy is again concentrated around 8 MHz. Of the 3 repeat measurements made on this waveform, the average peak values were +23 and -23 millivolts.

Figures 32 and 33 show the transient observed on Circuit 3 with the NWDC in the wire configuration. The signal magnitude is now about 20 times greater than the noise, and the transient energy is concentrated about 5.6, 2.4 and 10.4 MHz. Nine repeat measurements were made on this transient, with the average peak values being +159 and -199 millivolts.

The transients on Circuit 3 increased in magnitude by 550 to 760 percent in changing from the fiber optics to wire configurations. In addition, the bulk of the transient energy shifted from 8 MHz to 5.6, 2.4, and 10.4 MHz.

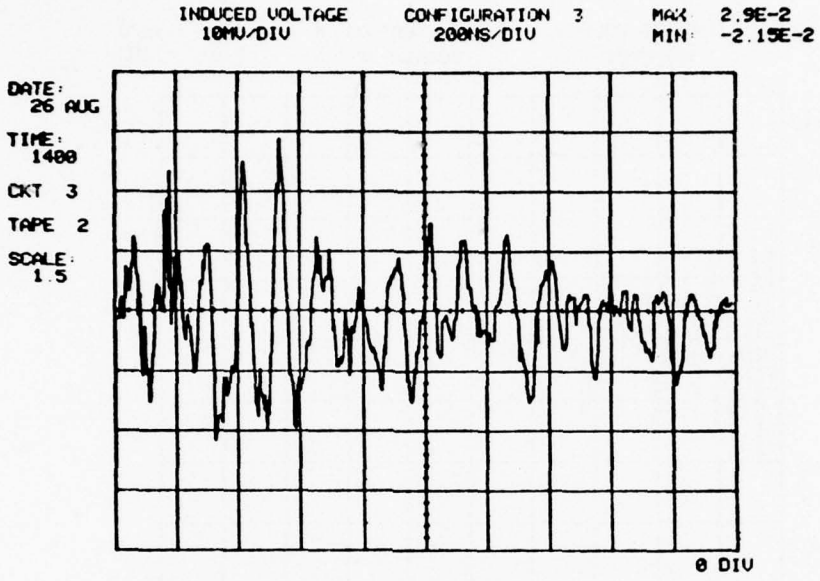

FIGURE 30. Induced Transient, Circuit 3,
Fiber Optics Configuration (#3)

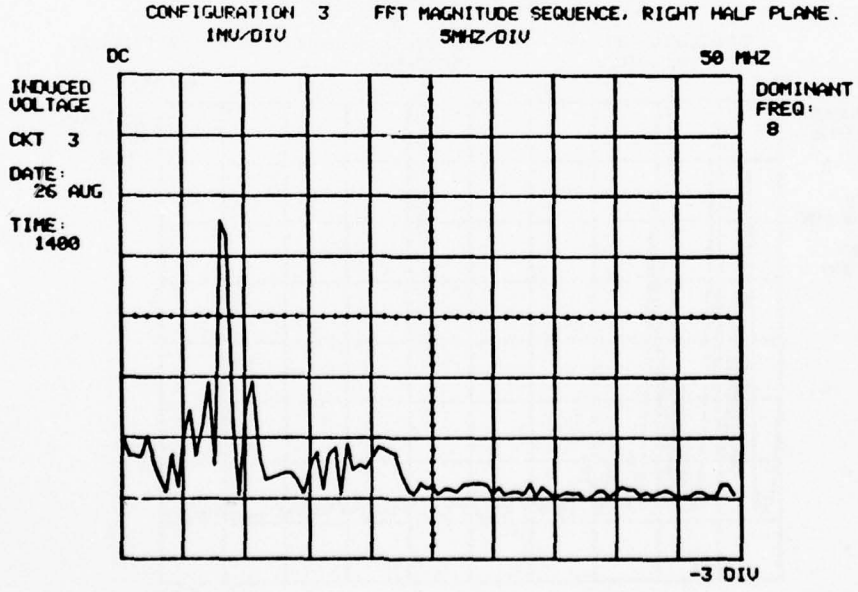

FIGURE 31. Frequency Spectrum, Circuit 3
Fiber Optics Configuration (#3)

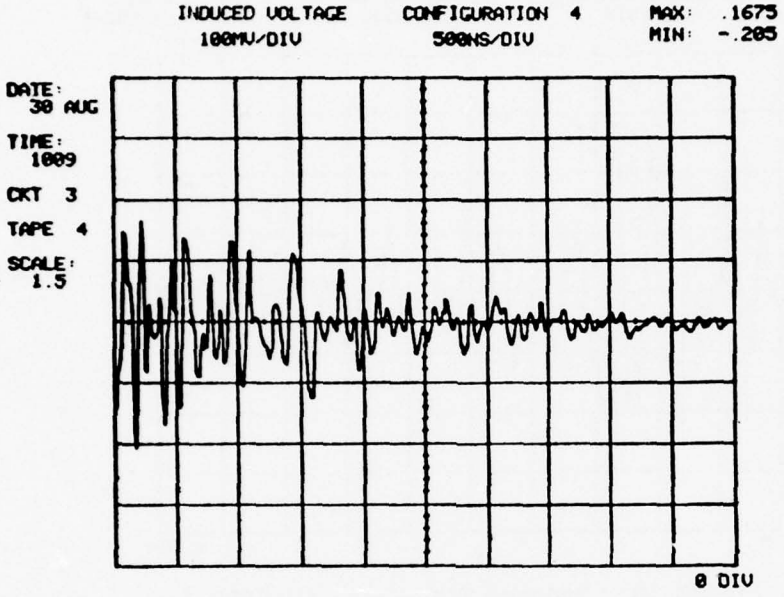

FIGURE 32. Induced Transient, Circuit 3, Wire Configuration (#4)

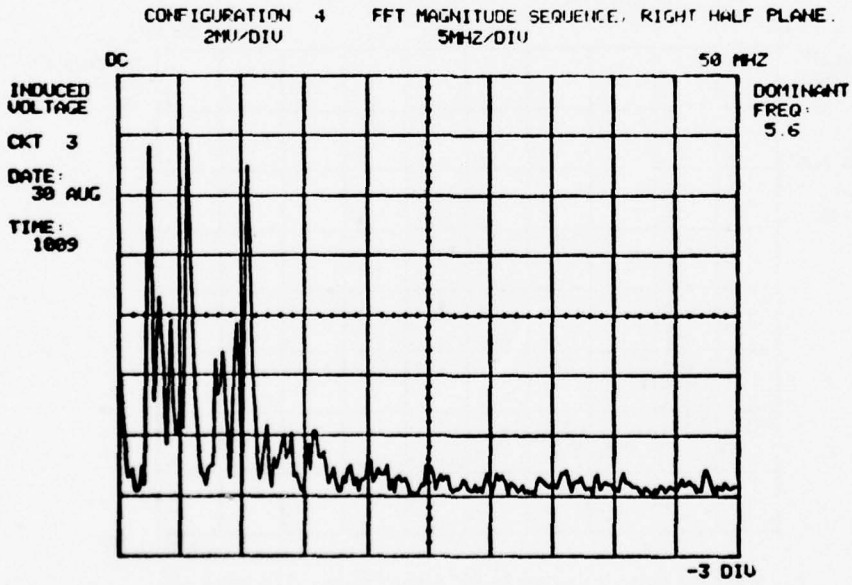

FIGURE 33. Frequency Spectrum, Circuit 3, Wire Configuration (#4)

4.1.4 +5 VDC Power (Circuit 6). Figures 34 and 35 show a typical transient observed on Circuit 6 with the NWDC in the fiber optics configuration. (In order to enhance the RF portions of the frequency spectrum, the large DC component was eliminated from the signal before the Fourier Transform was computed.) Of the 6 repeat measurements made on this waveform the average peak values were +30 and -131 millivolts. Notice in Figure 34 that the RF peak magnitude is significantly greater than the underlying DC pulse. Figure 35 shows that the major frequency components in the RF portion of the transient were 2.1 and 4.2 MHz. Though not shown well in this figure, the major low frequency component of the pulse was at about 80 KHz.

Figures 36 through 38 show a typical transient observed with the NWDC in the wire configuration. Note that Figure 36 shows only the leading edge of the full transient shown in Figure 38 at a slower sweep speed. Notice in Figure 36 that RF portion of the transient is now significantly lower in magnitude than the underlying low frequency pulse. This is a change from Configuration 3. The spectrum of this pulse also shows that now the transient energy has more of a noise character, also a change from the fiber optics configuration. Figure 38 shows the overall pulse shape and magnitude, and a total of 7 repeat measurements were made on this transient. The average peak values were +24 and -92 millivolts.

Though not shown, it was observed that the circuit was responding with an overall pulse shape similar to that shown in Figure 38 even in the fiber optics configuration. Thus, the net change between the fiber

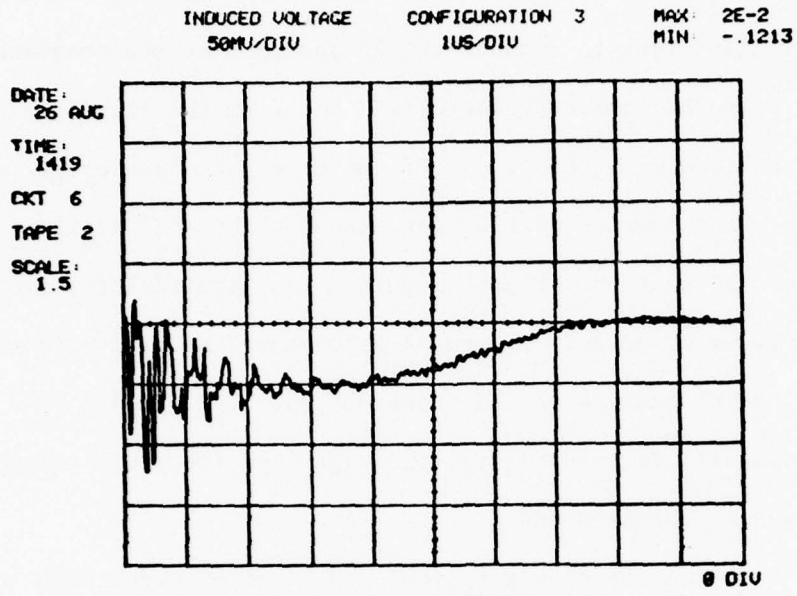

FIGURE 34. Induced Transient, Circuit 6,
Fiber Optics Configuration (#3)

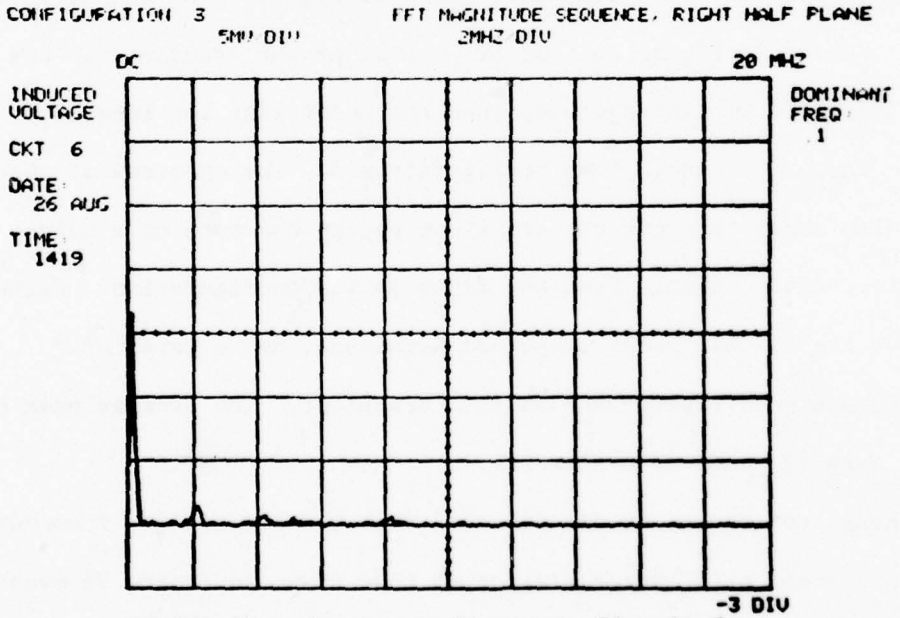

FIGURE 35. Frequency Spectrum, Circuit 6,
Fiber Optics Configuration (#3)

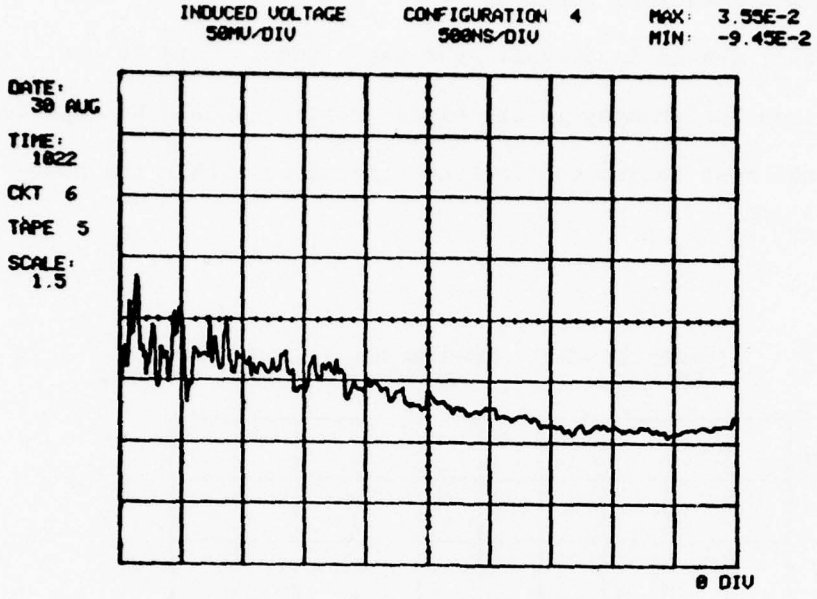

FIGURE 36. Induced Transient, Circuit 6, Wire Configuration (#4)

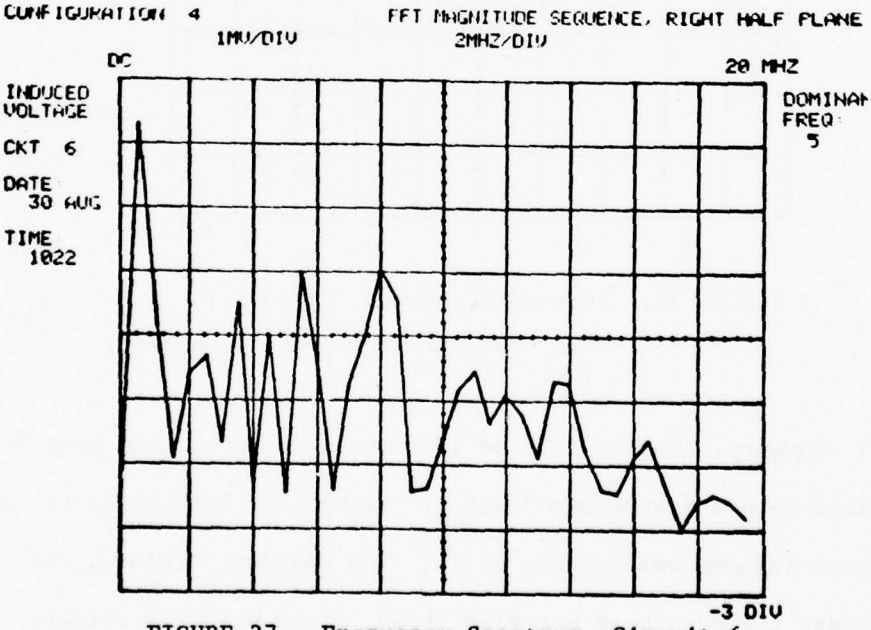

FIGURE 37. Frequency Spectrum, Circuit 6, Wire Configuration (#4)

optics and wire configurations was a shift in the relative magnitudes of the RF and low frequency portions of the transient pulse, with relatively little change in overall peak magnitudes. This is not surprising, since the changes in the signal cabling should be expected to have only the most indirect effect on transients within the power supply circuitry.

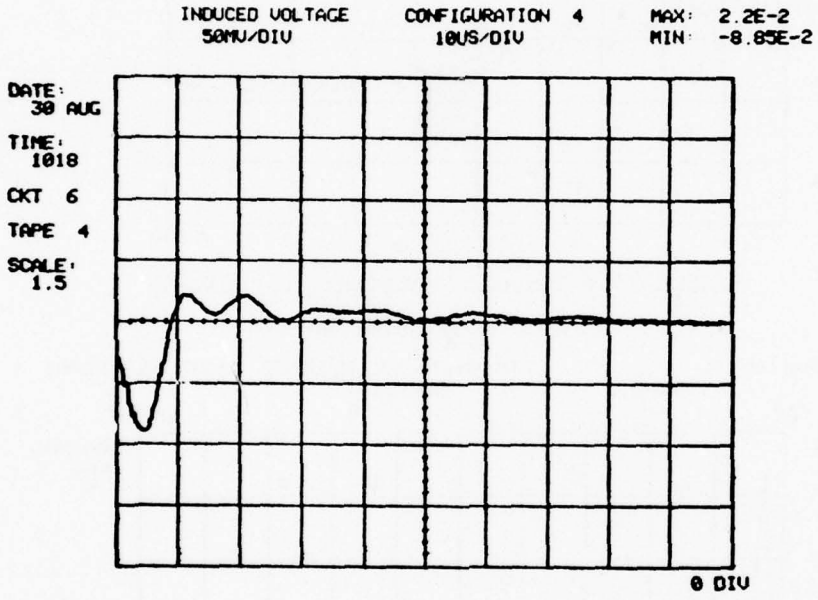

FIGURE 38. Induced Transient, Circuit 6, Wire Configuration (#4), Slow Sweep

4.1.5 Summary. Tables III and IV summarize the induced transient data obtained in Configurations 3 and 4. Values for both positive and negative peak induced voltage are given. The maximum, minimum, and average values for each peak are also shown, along with the primary frequencies present in the signal spectra.

All signals showed a marked difference in frequency spectrum between the fiber optics and wire configurations. The data circuits all showed large increases in induced voltage when changing from the fiber optics to hard-wire configuration. These increases ranged from 550% (circuits 1 & 3) to 810% (circuit 2).

The spectrum of the transients observed on the power supply circuit changed between configurations 3 and 4, but the peak magnitudes changed relatively little (about 40%), and this increase occurred in changing from the wire to fiber optics configuration. In the fiber optics configuration the RF components in the transient were larger than the low frequency components, while in the wire configuration, the reverse was true. These results were most likely due to the fact that some power ground returns were included in the signal cabling, so connecting and disconnecting the signal cables did modify the power supply circuits somewhat.

TABLE III. Fiber Optics Data Summary

CIRCUIT	# DATA POINTS	PEAK INDUCED VOLTAGE MAX VALUE (mV)	MIN VALUE (mV)	AVG VALUE (mV)	PRIMARY FREQS (MHz)
1	4	+37 -28	+21 -25	+26 -26	8
2	4	+49 -40	+37 -30	+42 -36	8
3	3	+29 -24	+18 -21	+23 -23	8
6	6	+42 -143	+20 -120	+30 -131	80 KHz, 2.1, 4.2

TABLE IV. Hard-wire Data Summary

CIRCUIT	# DATA POINTS	PEAK INDUCED VOLTAGE MAX VALUE (mV)	MIN VALUE (mV)	AVG VALUE (mV)	PRIMARY FREQS (MHz)
1	8	+200 -223	+127 -145	+171 -179	2.4, 4.2
2	8	+410 -384	+356 -291	+382 -336	0.9
3	9	+170 -255	+150 -120	+159 -199	5.6, 2.4 10.4
6	7	+35 -95	+16 -89	+24 -92	80 KHz, 8, 5.4

4.2 Coupling Mechanism Comparison

To draw a comparison on the relative importance of the three coupling mechanism, measurements were made on the NWDC circuits in three simplified configurations (8, 7, and 5) which isolated each of the three coupling mechanisms.

4.2.1 NWDC. When in Configuration 8, the NWDC had no external wires connected to it. The induced measurements made in this configuration then show the amount of energy being coupled directly into the NWDC circuits. Figures 39 and 40 show a typical transient measurement made in this configuration. This waveform is an example of those observed on Circuit 2, but as can be seen in Table V, the transients observed on Circuits 1 and 3 were very similar in magnitude and frequency content to those on Circuit 2.

The waveform is very similar to transients observed with the NWDC in the fiber optics configuration, and also very similar to the noise measurements, though about 3 times greater in magnitude. Most of the transient energy is concentrated about 8 MHz. Table V summarizes the data obtained on all three circuits in this configuration. In all cases the bulk of the energy was concentrated around 8 MHz, with peak time-domain magnitudes 2 to 3 times greater than the noise measurements.

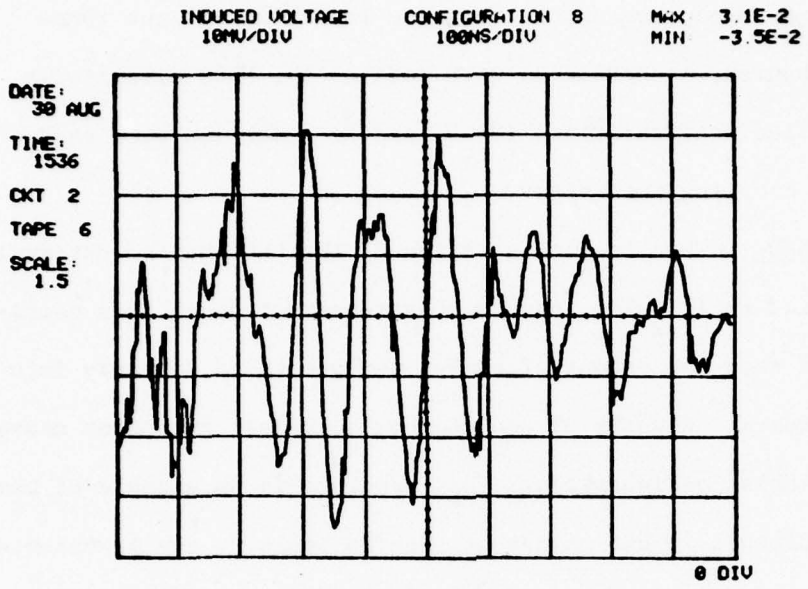

FIGURE 39. Induced Transient, Configuration 8

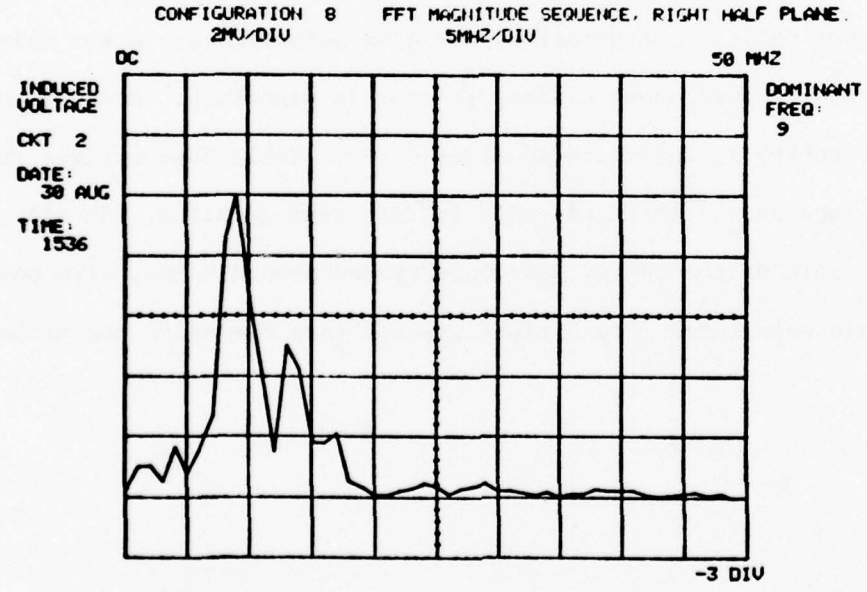

FIGURE 40. Frequency Spectrum, Configuration 8

TABLE V. Configuration 8 Induced Data

CIRCUIT	# DATA POINTS	PEAK INDUCED VOLTAGES MAX VALUE (mV)	MIN VALUE (mV)	AVG VALUE (mV)	PRIMARY FREQS (MHz)
1	6	+29	+18	+23	8
		-22	-34	-26	
2	6	+50	+28	+35	9
		-40	-35	-38	
3	7	+31	+18	+25	8
		-35	-22	-29	

4.2.2 Hard-wire Signal Cabling. When in Configuration 7, the NWDC had only the hard-wire signal wiring connected. Power cabling was not connected. Compared to the results obtained in Configuration 8, transients on all three circuits were much greater in magnitude, and very different in frequency content.

Figures 41 and 42 show a typical transient observed on Circuit 1 in this configuration. The peak magnitude is approximately 480% greater than that observed in Configuration 8, and most of the transient energy is now concentrated around 2.2 and 4.2 MHz rather than at 8 MHz as was the case in Configuration 8. Seven measurements were made on this transient, and the average peak values were +133 and -120 millivolts.

Figures 43 and 44 show a typical transient observed on Circuit 2 in this configuration. This waveform averaged about 3 times greater in magnitude than that observed in configuration 8, and much transient energy now appears at 22.5, 11, and 16 MHz. A total of 7 repeat measurements were made of this transient, and the average peak values were +91 and -91 millivolts. The major frequency components were 22.5, 11, and 16 MHz.

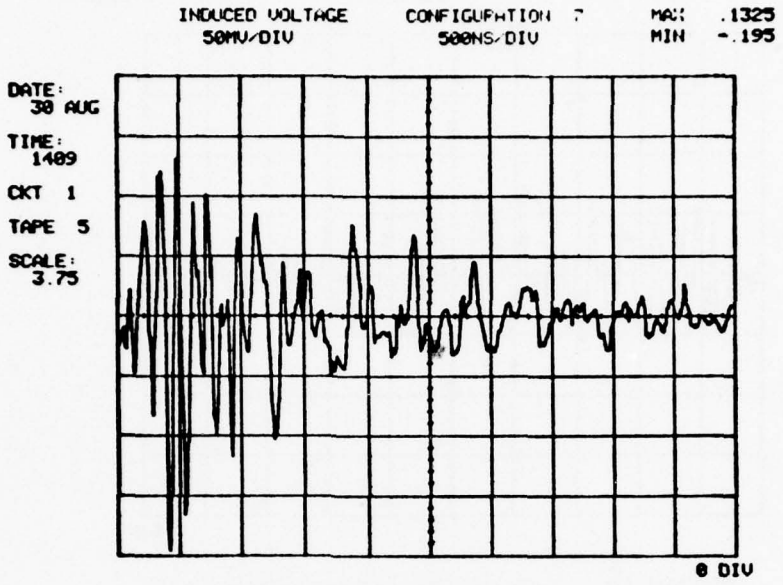

FIGURE 41. Induced Transient, Circuit 1, Configuration 7

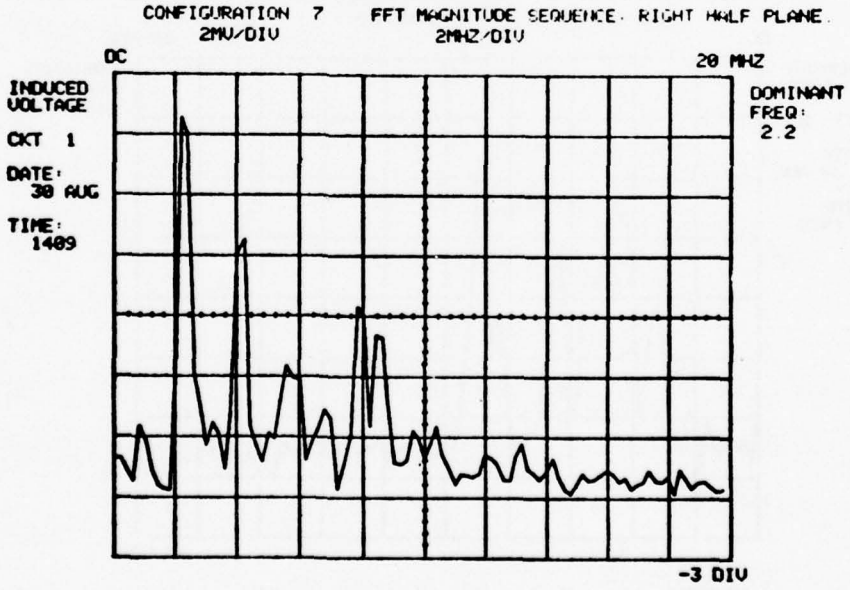

FIGURE 42. Frequency Spectrum, Circuit 1, Configuration 7

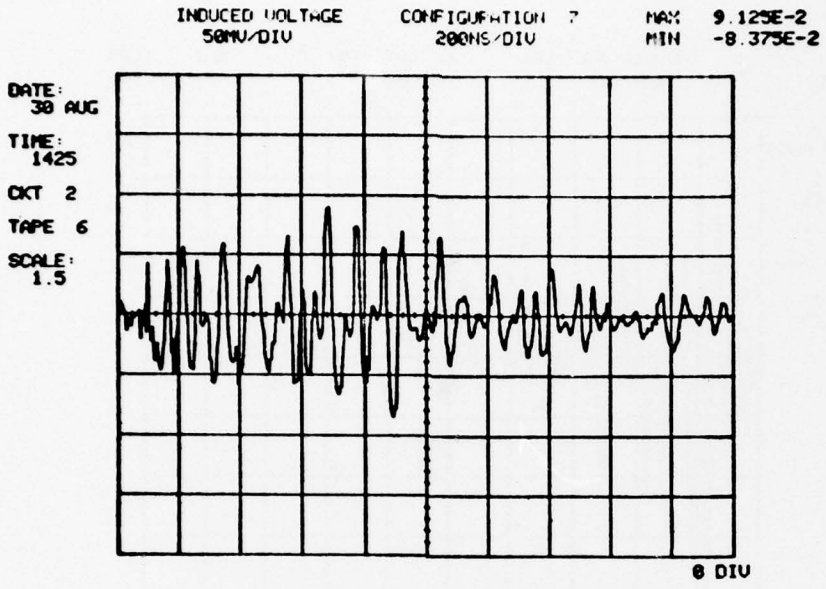

FIGURE 43. Induced Transient, Circuit 2, Configuration 7

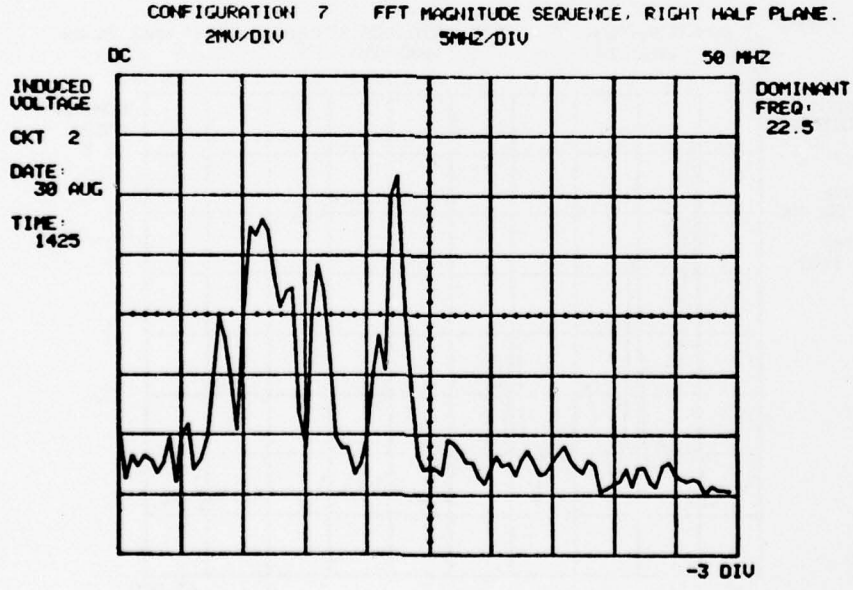

FIGURE 44. Frequency Spectrum, Circuit 2, Configuration 7

Figures 45 and 46 show a typical transient observed on Circuit 3 in this configuration. The peak magnitude of this waveform is about 6 times that of the transient observed in Configuration 8, and the major frequency components are 5.8, 2.2, and 11 MHz. A total of 8 repeat measurements were made on this transient, and the average peak values were +175 and -199 millivolts.

Table VI summarizes the data obtained in Configuration 7. The transients on each circuit increased 160 to 600 per cent with major changes in frequency content also. This shows, as is reasonable to expect, that the effect of adding signal wiring to the system greatly increases the transient levels, and also greatly changes their nature.

TABLE VI. Configuration 7 Induced Effects Data

		PEAK INDUCED VOLTAGE			
CIRCUITS	# DATA POINTS	MAX VALUE (mV)	MIN VALUE (mV)	AVG VALUE (mV)	PRIMARY FREQS (MHz)
1	7	+138 -244	+124 -178	+133 -210	2.2, 4.2
2	7	+111 -109	+56 -70	+91 -90	22.5, 11, 16
3	8	+190 -239	+142 -173	+175 -199	5.8, 2.2, 11

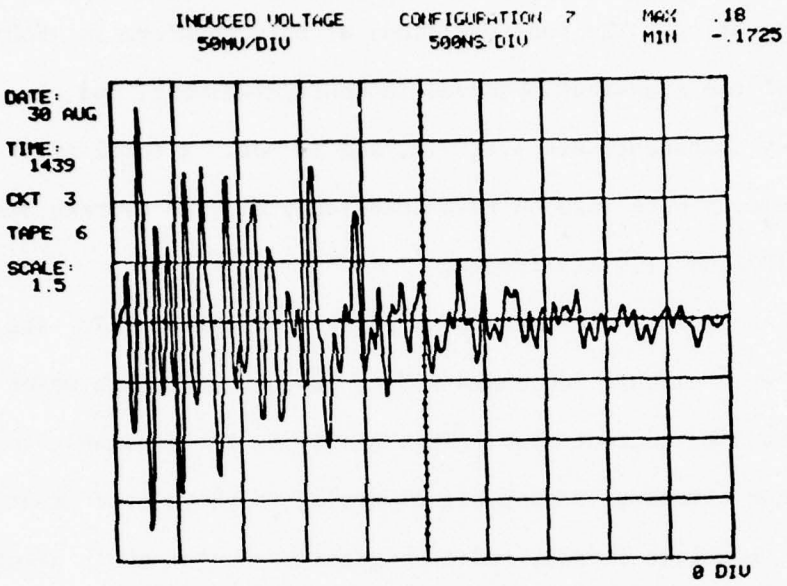

FIGURE 45. Induced Transient, Circuit 3, Configuration 7

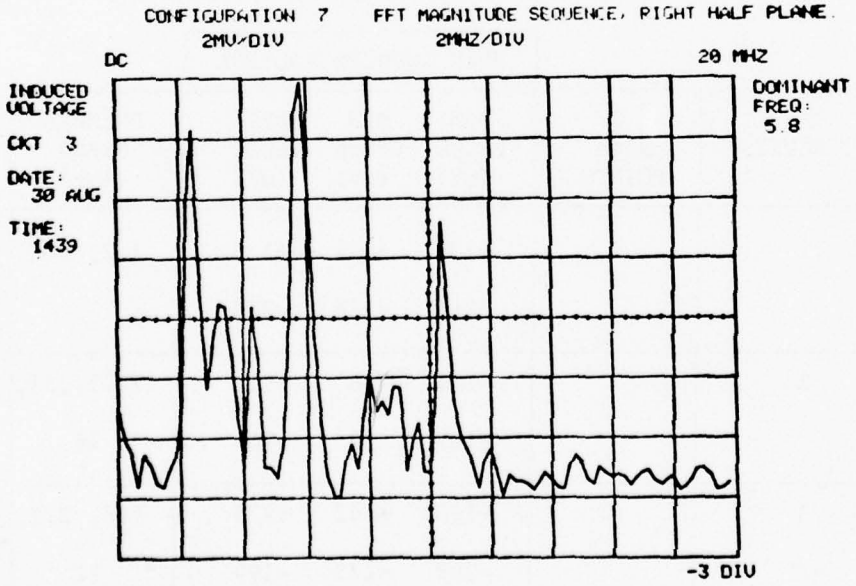

FIGURE 46. Frequency Spectrum, Circuit 3, Configuration 7

4.2.3 Power Cabling. When in Configuration 5, the NWDC had only its power cabling connected. In two of the three circuits, the transients in this configuration were only slightly greater in magnitude than those observed in Configuration 8 -- this was as expected. Circuit 2, however, experienced transients 15 times greater in magnitude than it did in Configuration 8.

Figures 47 and 48 show a typical transient observed on Circuit 1 in this configuration. The peak magnitudes are about twice those observed in Configuration 8, but the frequency content is quite different. Eight repeat measurements were made on this signal, and the average peak values were +58 and -59 millivolts. The major frequency components were 10.4, 8 and 4.2 MHz.

Figures 49 and 50 show a typical transient observed on Circuit 2 in this configuration. These transients were about 15 times greater than those observed in Configuration 8. A total of ten repeat measurements were made on this transient, and the average peak values were +554 and -427 millivolts. The only major frequency component was 4.2 MHz. This transient was also about 6 times greater in magnitude than that observed on this circuit in Configuration 7.

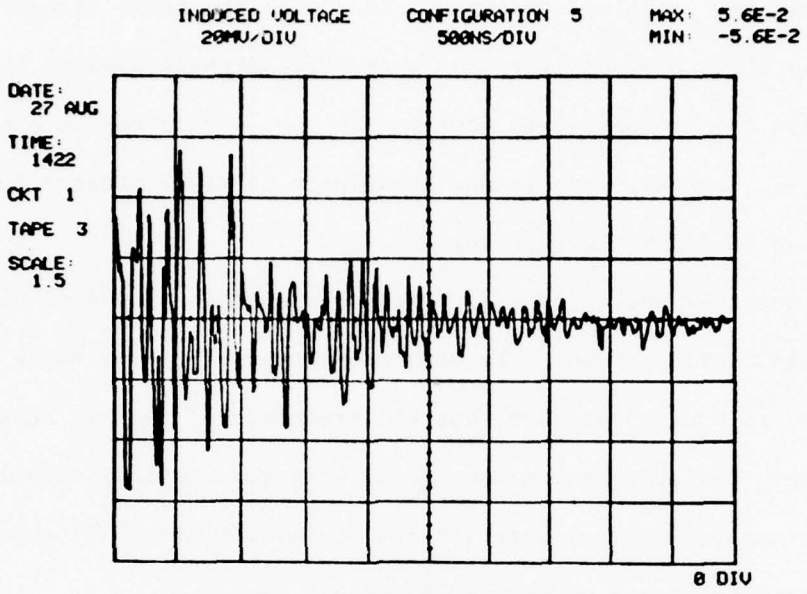

FIGURE 47. Induced Transient, Circuit 1, Configuration 5

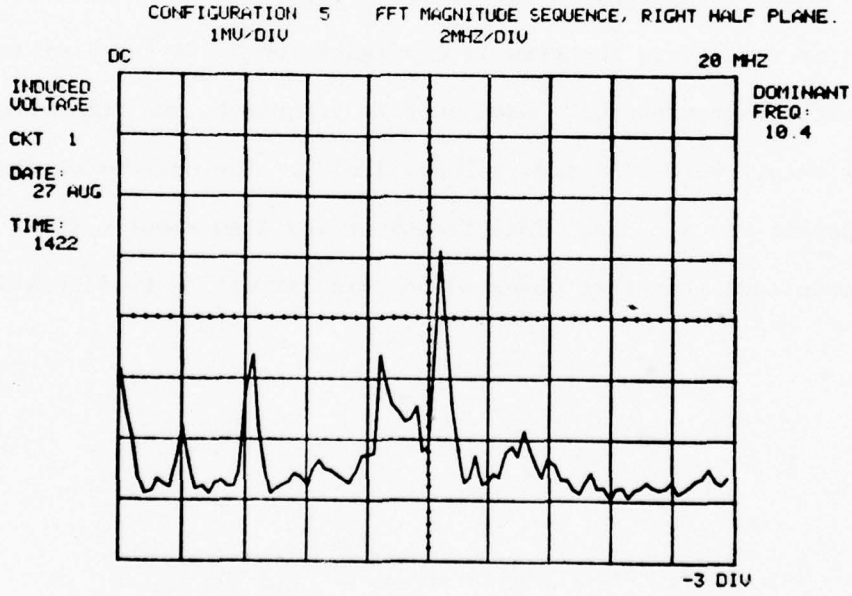

FIGURE 48. Frequency Spectrum, Circuit 1, Configuration 5

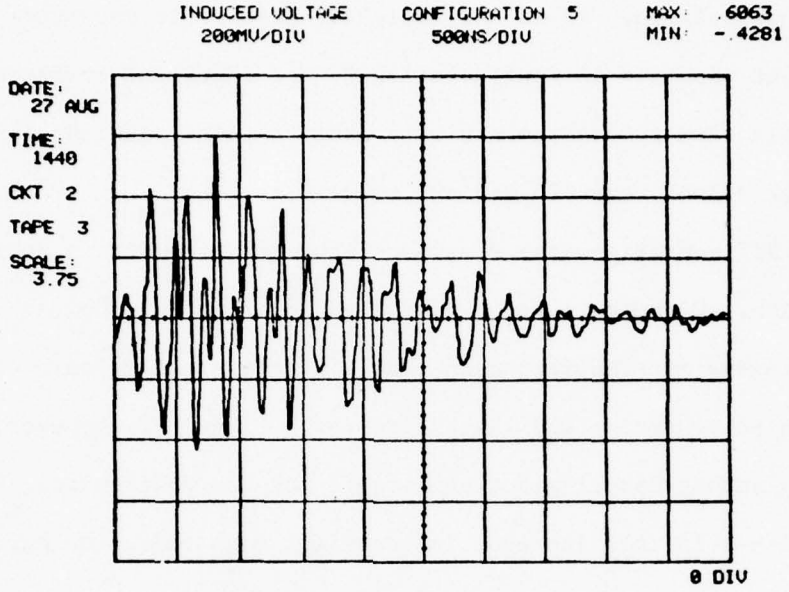

FIGURE 49. Induced Transient, Circuit 2, Configuration 5

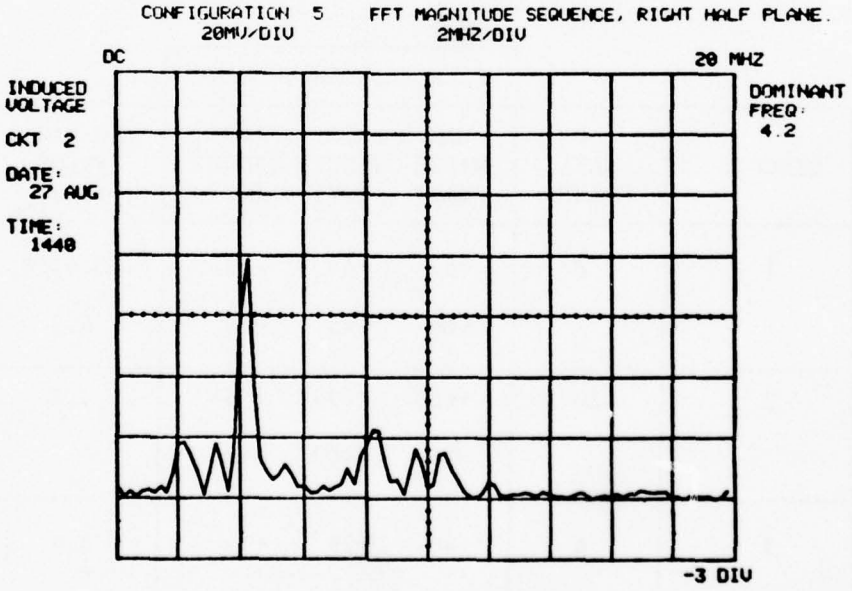

FIGURE 50. Frequency Spectrum, Circuit 2, Configuration 5

Figures 51 and 52 show a typical transient observed on Circuit 3 in this configuration. It is only slightly greater in magnitude than the transient observed in Configuration 8, and identical in frequency content. Six repeat measurements were made on this transient, and the average peak values were +35 and -47 millivolts.

Table VII summarizes the results of the measurements in this configuration. Circuits 1 and 3 performed as expected, showing only slight increases in transient magnitude, indicating only loose coupling between the power wiring and these circuits. Circuit 2, however, displayed very strong coupling between itself and the power wiring by reacting with a 15-fold increase in transient magnitude. No explanation is offered for this strong apparent coupling.

TABLE VII. *Configuration* 5 Induced Effects Data

		PEAK INDUCED VOLTAGE			
CIRCUIT	# DATA POINTS	MAX VALUE (mV)	MIN VALUE (mV)	AVG VALUE (mV)	PRIMARY FREQS (MHz)
1	8	+67 -68	+44 -45	+58 -59	10.4, 8, 4.2
2	10	+653 -484	+294 -400	+554 -427	4.2
3	6	+40 -52	+29 -43	+35 -47	8.5

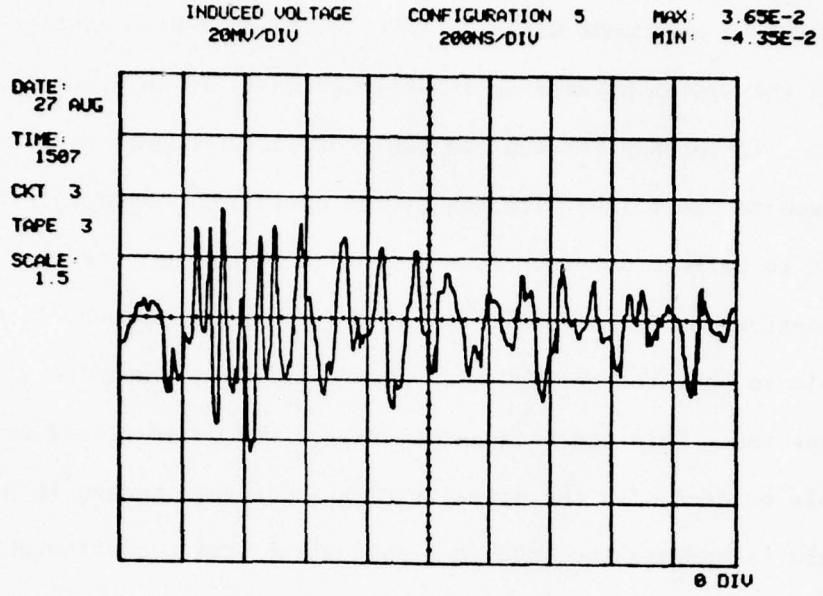

FIGURE 51. Induced Transient, Circuit 3, Configuration 5

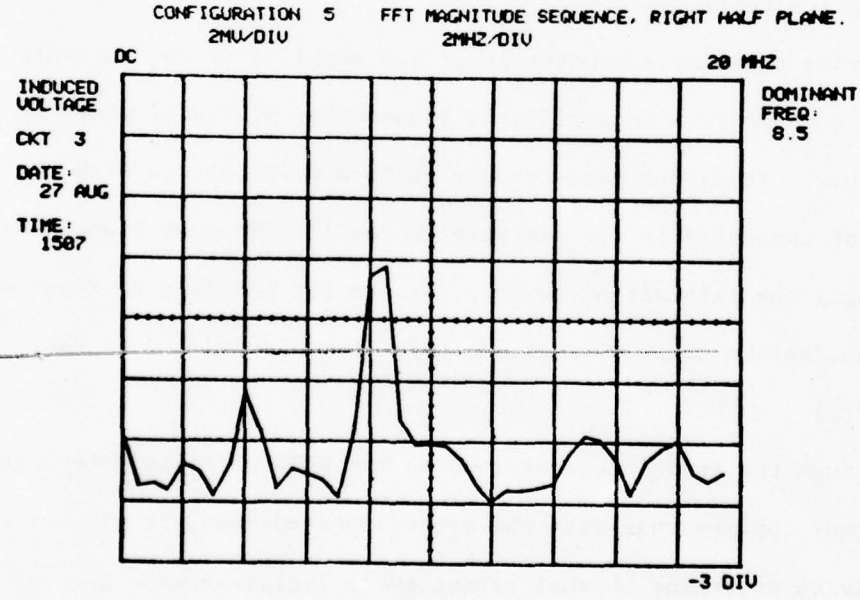

FIGURE 52. Frequency Spectrum, Circuit 3, Configuration 5

4.3 Power-On Measurements

Measurements were made with the NWDC in the hard-wire configuration with the system powered-up (Configuration 6) in an attempt to establish a relationship between the power-off measurements and what might be expected in flight with the system operating. Although it was desired to perform power-on measurements in both the hard-wire and fiber optics configurations to yield a further comparison, it was not possible to operate the NWDC with power applied and no wire signal cables connected. This was because several of the power ground returns shared cable bundles with the signal wiring. For this reason it was not possible to operate the NWDC in a pure fiber optics configuration with power applied. (In flight, with the ALOFT NWDS, the wire signal cabling is connected to the NWDC even when operating the system in the fiber optics configuration.)

During these measurements power was supplied to the aircraft through a cable from an unfiltered transformer providing power to the hangar. Transient measurements on this power source with the cable not connected to the aircraft showed 15-Volt peak transients overriding the 115-Volt AC power. (It was not possible to measure the transients on the power cable while it was connected to the aircraft.)

Though the transients observed on the NWDC circuits were higher with power applied than with the system powered-down, it was not possible to determine to what extent these increases were due to additional transient energy entering the aircraft via the power

cable -- either through indirect coupling with the signal circuits or directly through the power supply circuits within the NWDC.

The results of the power-on measurements are included here as observations, but due to the foregoing conditions, it cannot be concluded that transients of these magnitudes will be experienced under flight conditions. The observed transients were most probably somewhat more severe than those that might be expected in flight.

4.3.1 Circuit 1. Figures 53 and 54 show a typical transient observed on Circuit 1 with power applied. The signals were greater in magnitude than those observed without system power by about 450%. Frequency content was similar. Six repeat measurements were made on this circuit, and the average peak values were +932 and -876 millivolts. The primary frequencies were 5.4 and 2.2 MHz.

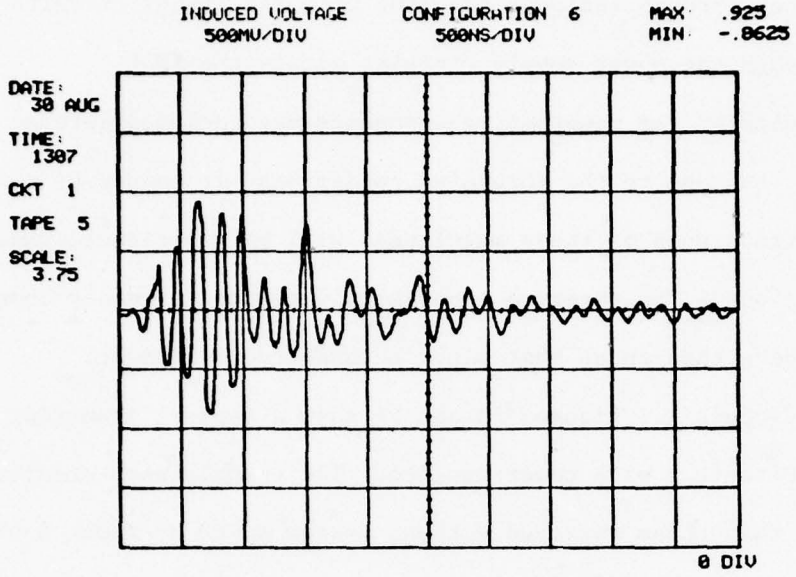

FIGURE 53. Induced Transient, Circuit 1, Power On

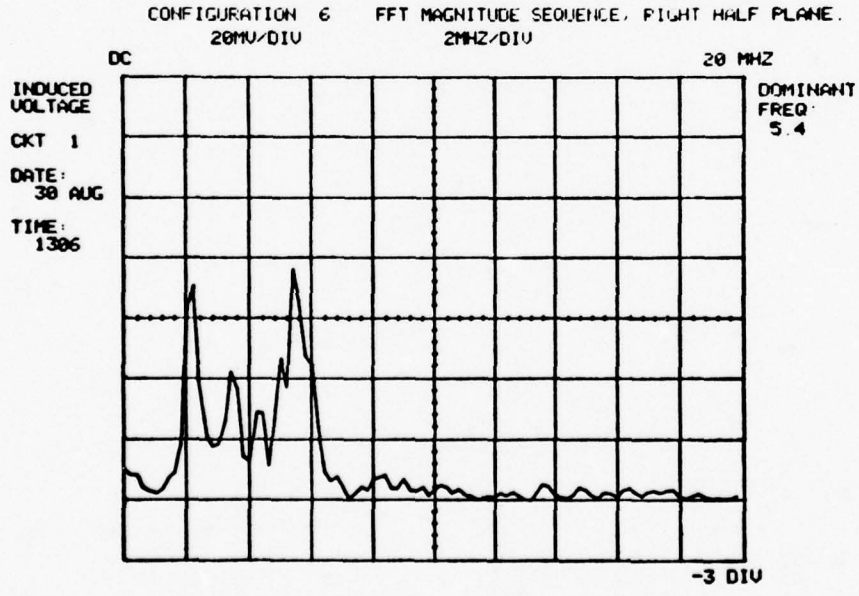

FIGURE 54. Frequency Spectrum, Circuit 1, Power On

4.3.2 Circuit 2. Figures 55 and 56 show a typical transient observed on Circuit 2 with power applied. Note that the transient is displaced by a DC level due to the data signal being sent by the NWDC. The amounts of DC offset were considered in interpreting the data, and the magnitudes listed in the summary table reflect only the transient magnitudes. Five repeat measurements were made on this waveform, and the average peak values were +1.21 and -1.39 Volts. This represented a 300% increase over the values obtained in Configuration 4 with power off. The two primary frequency components were 3.4 and 2.1 MHz.

4.3.3 Circuit 3. Figures 57 and 58 show a typical transient observed on Circuit 3 with power on. Four repeat measurements were made on this circuit, and the average peak transient magnitudes were +.98 and -1.19 Volts. Primary frequency components were 2.2 and 5.4 MHz. These magnitudes represented an approximate 600% increase over the transients observed with power off.

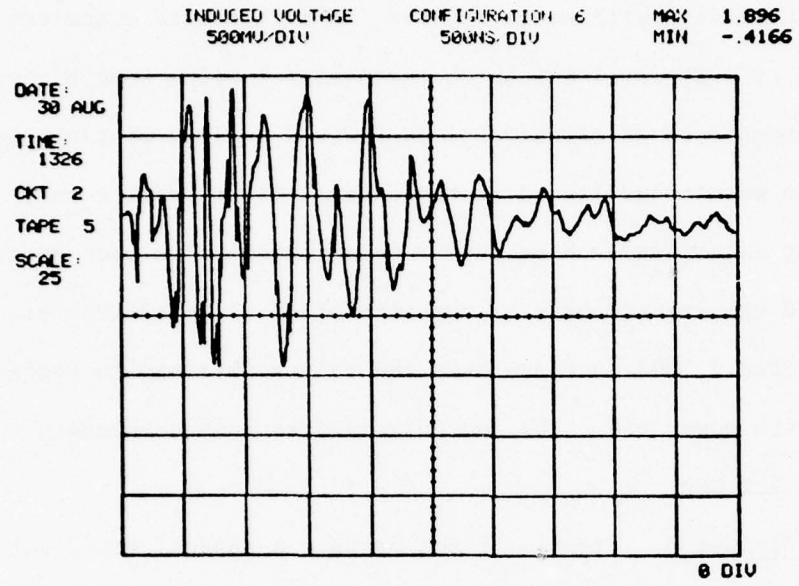

FIGURE 55. Induced Transient, Circuit 2, Power On

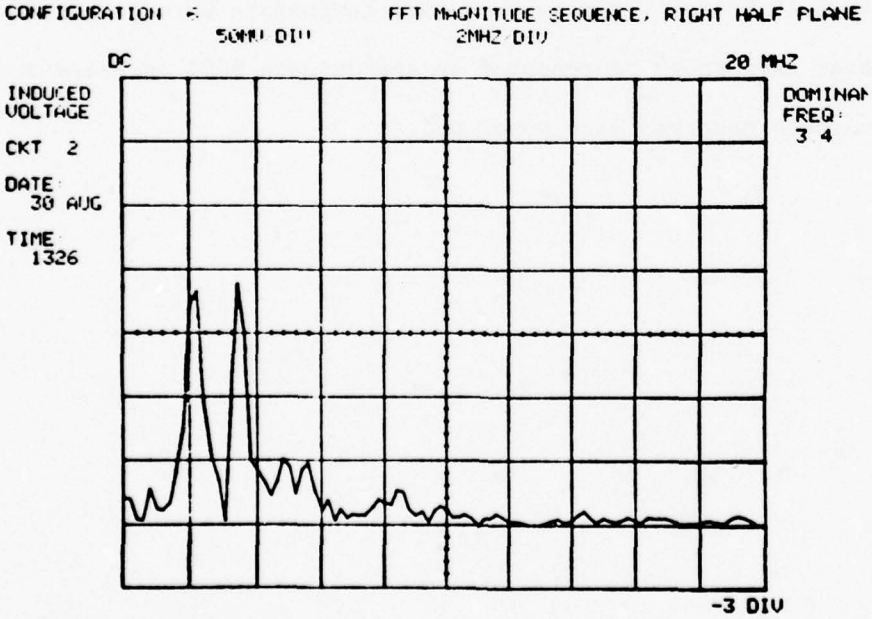

FIGURE 56. Frequency Spectrum, Circuit 2, Power On

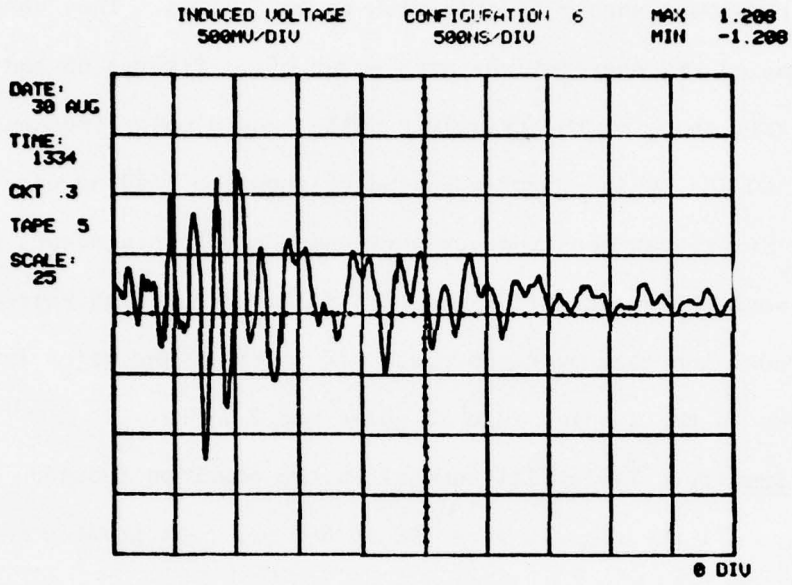

FIGURE 57. Induced Transient, Circuit 3, Power On

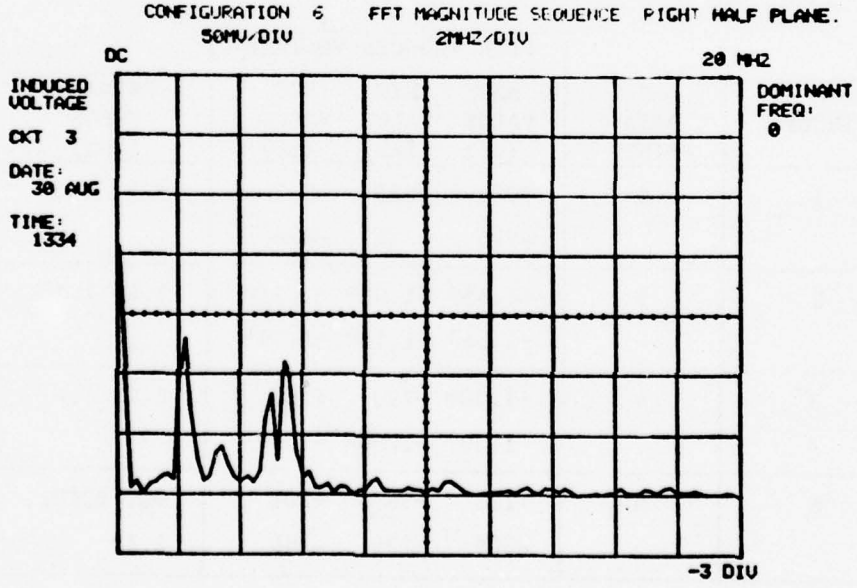

FIGURE 58. Frequency Spectrum, Circuit 3, Power On

4.3.4 Circuit 6. Figures 59 through 62 show a typical transient observed on the power supply circuit with power applied. They very closely resembled the observations with power off. Figures 63 and 64 show the overall shape of the transient pulse, and a major frequency component of 80 KHz, while Figures 65 and 66 show the leading edge of this pulse. Six repeat measurements were made on this transient, and the average peak values were +101 and -266 millivolts, which represents less than a 300% increase over the power-off values. The major frequency present in the leading-edge RF noise was 2.1 MHz.

4.3.5 Summary. Table VIII summarizes the power-on induced measurements. All the signals were 300 to 600 per cent greater than the corresponding power-off measurements.

TABLE VIII. Power-On Measurements

CIRCUIT	# DATA POINTS	PEAK INDUCED VOLTAGE MAX VALUE (mV)	MIN VALUE (mV)	AVG VALUE (mV)	PRIMARY FREQS (MHz)
1	6	+981 -975	+863 -731	+932 -876	5.4, 2.2
2	5	+1.45* -1.56*	+1.06* -1.19*	+1.21* -1.39*	3.4, 2.2
3	4	+1.20* -1.20*	+790 -1.06*	+982 -1.19*	2.2, 5.4
6	6	+128 -306	+56 -224	+101 -266	DC, 80KHz, 2.1

* These values are in Volts.

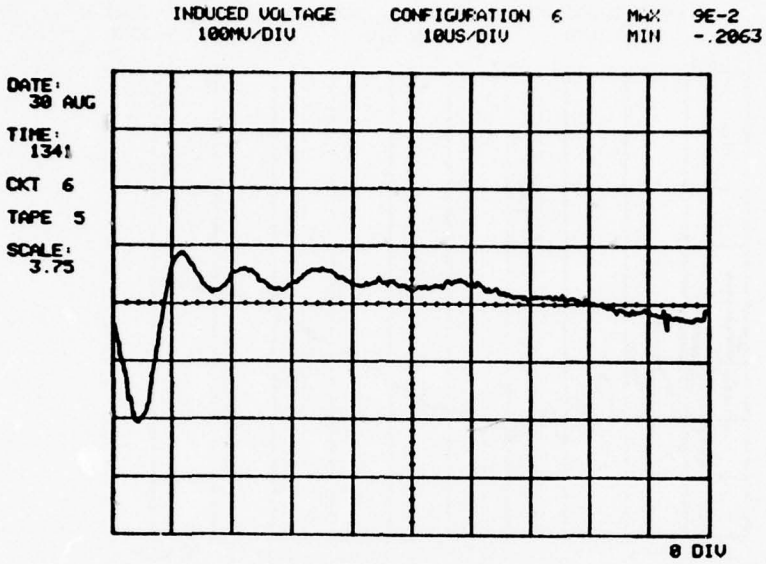

FIGURE 59. Induced Transient, Circuit 6, Power On, Slow Sweep

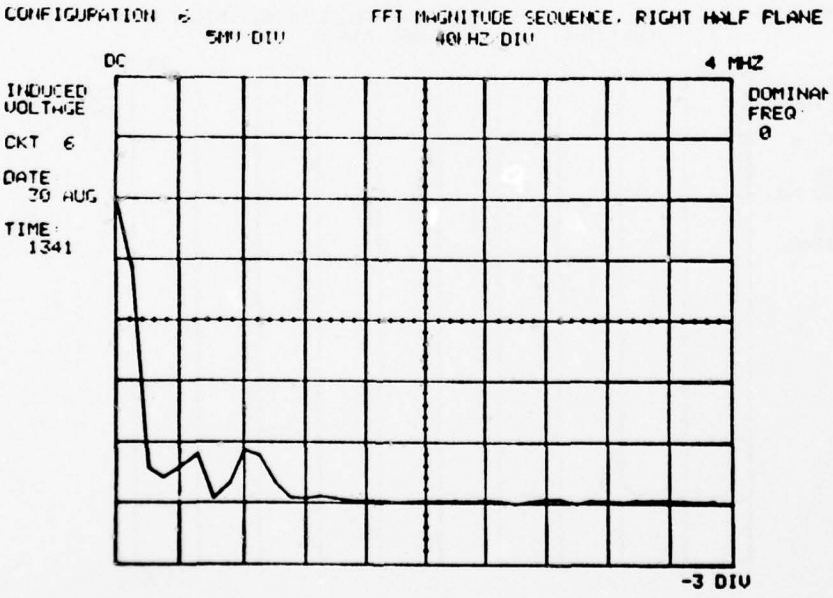

FIGURE 60. Frequency Spectrum, Circuit 6, Power On, Low Frequency

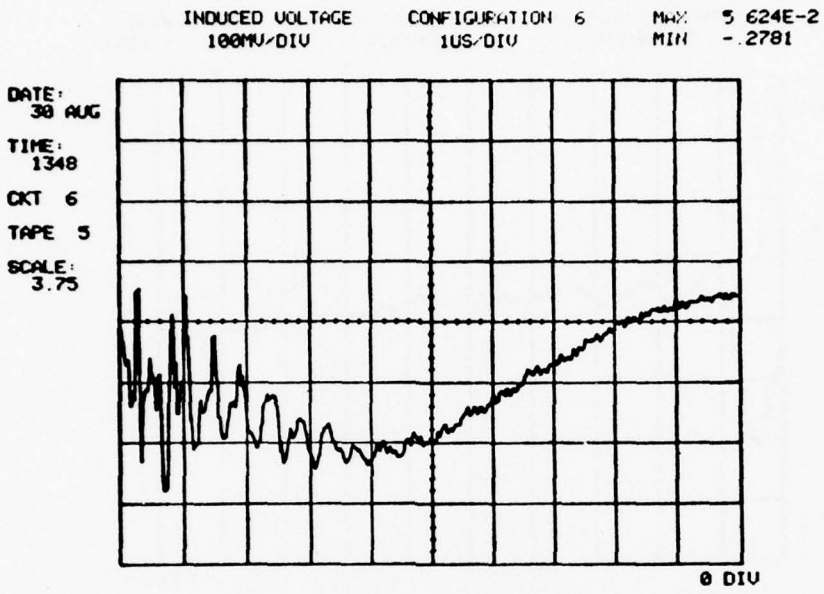

FIGURE 61. Induced Transient, Circuit 6, Power On, Leading Edge

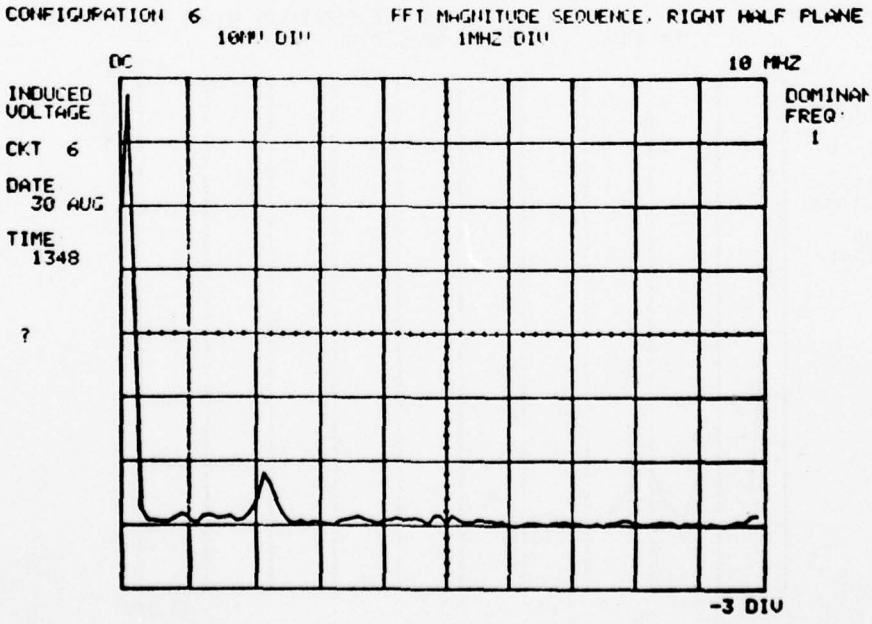

FIGURE 62. Frequency Spectrum, Circuit 6, Power On, High Frequency

4.4 Electro-optical Circuits

Measurements were made at two points within the electro-optical interface circuits in the NWDC in order to establish the levels and types of transients that would be experienced by these circuits. These measurements were made only with the NWDC in the fiber optics configuration, with power cabling connected.

4.4.1 NAV Panel Data Receiver Output. Figures 63 and 64 show a typical transient experienced by Circuit 4, the NAV Panel Data Receiver Output. The transients were very similar in magnitude and frequency content to those observed on the other circuits in Configuration 8, and also the noise measurements. A total of 4 repeat measurements were made on this circuit; the average peak values of the waveform were +19 and -14 millivolts.

4.4.2 NAV Panel Data Transmitter Input. Figures 65 and 66 show a typical transient observed on Circuit 5, the NAV Panel Data Transmitter Input. As might be expected, these signals were not significantly different from those observed on Circuit 4. Three repeat measurements were made, and the average peak values were +17 and -14 millivolts. The major frequency components were 8 and 17 MHz.

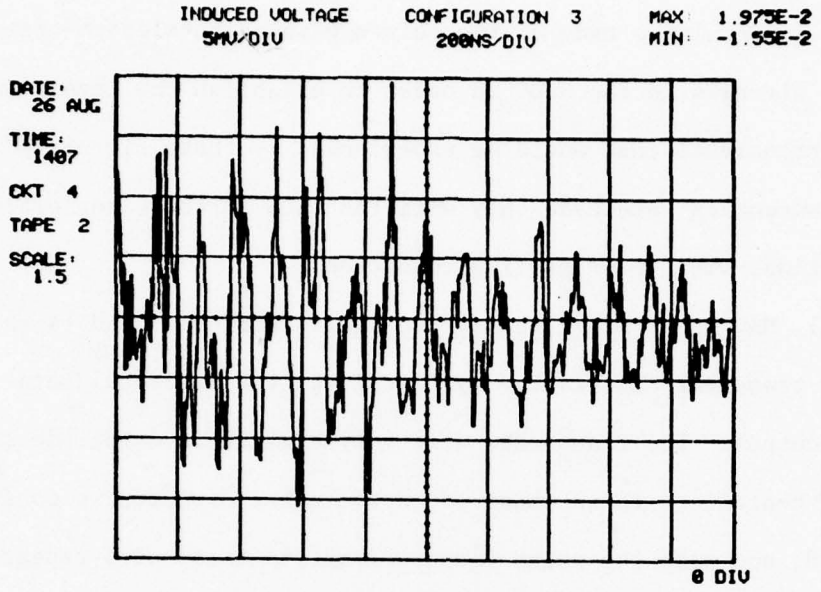

FIGURE 63. Induced Transient, Circuit 4

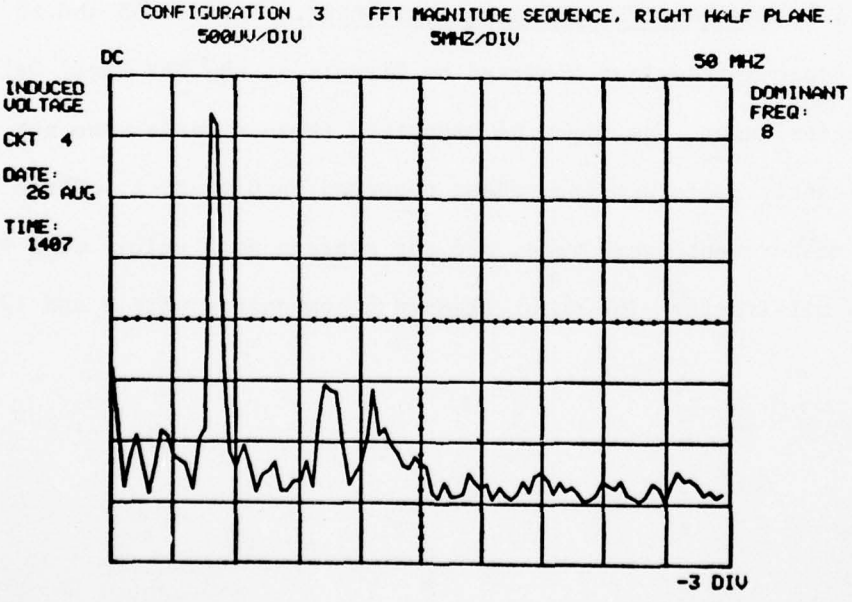

FIGURE 64. Frequency Spectrum, Circuit 4

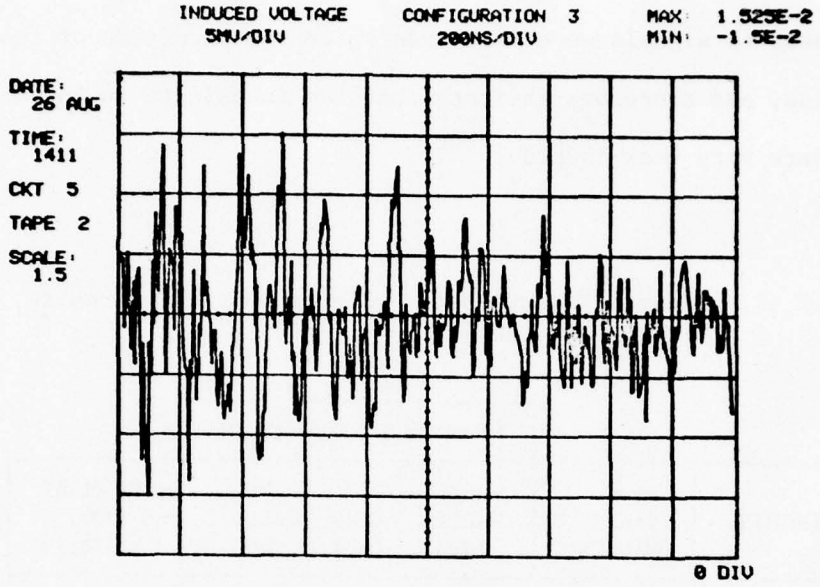

FIGURE 65. Induced Transient, Circuit 5

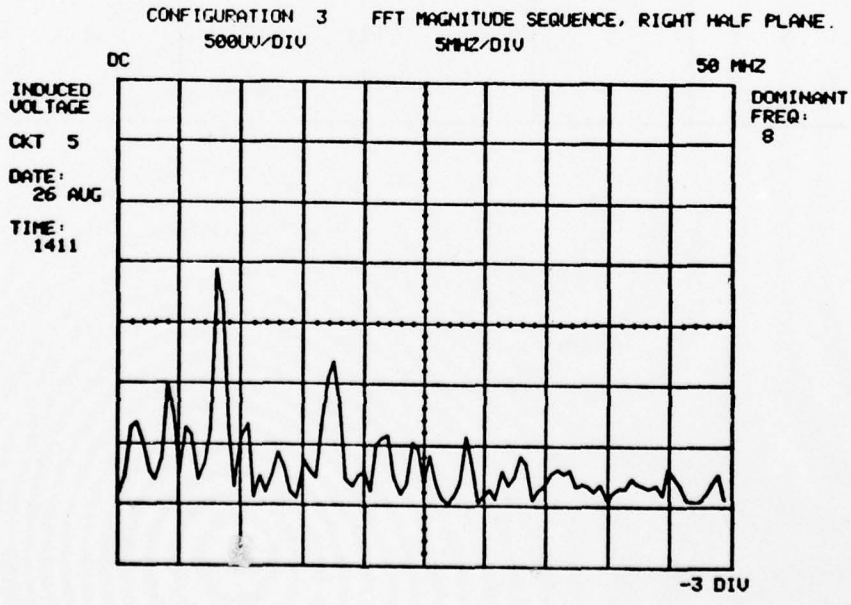

FIGURE 66. Frequency Spectrum, Circuit 5

4.4.3 Summary. Table IX summarizes the observations on these circuits. All measurements were made with the NWDC in Configuration 3. The observed signals were less than twice the magnitude of the system noise, and therefore indicate that the transients on these circuits were very weak indeed.

TABLE IX. Induced Effects Data - Electro-optical Circuits

		PEAK INDUCED VOLTAGE			
CIRCUIT	# DATA POINTS	MAX VALUE (mV)	MIN VALUE (mV)	AVG VALUE (mV)	PRIMARY FREQS (MHz)
4	4	+22 -15	+14 -13	+19 -14	8
5	3	+21 -12	+15 -16	+17 -14	8

5. SUMMARY AND CONCLUSIONS

5.1 Fiber Optics

Three data circuits within the Navigation and Weapons Delivery Computer were monitored for transients in both the fiber optics and hard-wire configurations. Transients observed in the hard-wire configuration were 550 to 810 per cent greater than those observed in the fiber optics configuration. The transients observed in the wire and fiber optics configurations also showed distinct differences in waveform and frequency content.

These results show that an 85 to 90 per cent reduction in transient magnitudes can be expected with the substitution of fiber optics data transmission links in a subsystem of this type. Since the NAV Panel circuit uses coaxial cable in the wire mode, and the FLR Signal Generator and HUD circuits use shielded twisted pairs (both considered relatively "hard" against induced transients), these results suggest that an even greater advantage would be gained by the use of fiber optics when compared to other wiring methods, such as unshielded wire bundles or unshielded twisted pairs.

Due to the arrangement of the ALOFT NWDS (discussed in detail in paragraph 1.2), it was not possible to obtain fiber optics versus wire comparison measurements at the receiver ends of any data channels; comparison measurements were only made at the data channel transmitter ends. Thus while this experiment did draw good comparisons between the fiber optics and wire channels, it is possible that some additional transient energy could be coupled through the optical transmitters and

allowed to corrupt the digital data in an operating system. This effect, if it exists, would not have been observed in this experiment. A fair estimate of this effect, however, can be made by interpretation of the transient levels observed at the optical driver (Circuit 5). Interpretation of this data by one familiar with the characteristics of the optical transmitter circuit should show to what degree additional transient energy might be transmitted by the driver.

The power supply circuit that was monitored in both configurations showed little significant change in transient magnitude when substituting the fiber optics for the wire signal cabling. The transients were composed of 80 KHz and RF (2 to 8 MHz) components. The magnitude of the 80 KHz component changed very little between the two configurations, while the magnitude of the RF components (of very short duration at the leading edge of the pulse) were greater in the fiber optics configuration than in the wire configuration. This response caused the overall peak transient magnitude to be 40% greater in the fiber optics configuration than in the wire configuration. In this type of circuit, however, the 80 KHz component (much greater in energy content than the RF components) is much more significant. For this reason, the transient threat to the power supply can be considered to be approximately the same in either configuration.

The change in the RF spectrum of the transients was most likely due to the fact that some power ground returns were included in the signal cabling connection. In changing from the wire to fiber optics

configuration the signal cabling was removed, eliminating these ground return connections and increasing the RF transients. This situation, however, would not be representative of a system exclusively designed for fiber optics operation.

5.2 Coupling Mechanisms

The transients observed on all three NWDC circuits with no cabling connected to the NWDC were never greater than 16% of the magnitude of the transients observed with the system fully cabled. This indicates that the bulk of the transient energy observed in the NWDC circuits was being coupled into the unit through the power and signal wiring. (The ALOFT NWDC is very well shielded; this type of comparison performed on other systems might show an even lower percentage of the total transient energy being coupled directly into the "black box".)

In two cases out of three (Circuits 1 and 3) the transients produced by the addition of the signal wiring to the NWDC were much greater (200 to 400 per cent) than those produced by the addition of the power wiring to the NWDC. This indicates a stronger coupling of the circuits to the signal wiring, as would be expected. This also suggests that the most effective way to reduce the transient levels in these circuits would be to reduce the transient energy entering the NWDC through the signal wiring (either by substituting fiber optics for the wires, or by adding transient suppression devices).

In one case, however (Circuit 2), the transients produced by the addition of the power wiring to the NWDC were 500% greater than those produced by the addition of the signal wiring. This suggests tight coupling to the power wiring for this circuit. This also suggests that the most effective way to reduce the transient levels on this circuit would be to reduce the coupling to the power wiring.

The conclusion regarding relative importance of these two coupling mechanisms (i.e., via power and signal wiring) must be, therefore, that they are both, in general, important, and their relative importance may vary from one circuit to another. While Circuit 2 showed the greatest coupling to the power wiring of the three data circuits, it also showed the greatest percentage reduction in transient magnitude with the substitution of fiber optics for the signal wiring. This indicates a rather tight and probably complex interdependence of both coupling mechanisms on the overall response of the circuit. On the other hand, while Circuit 2 did show the most improvement with the substitution of the fiber optics, it still showed the highest transient magnitudes even after substitution. This suggests that it might be possible to further reduce the transient levels by reducing the circuit coupling to the power wiring as indicated previously.

It is also interesting to note that in two cases out of three (Circuits 1 and 3), the transient magnitudes observed on the complete system were approximately equal to the sum of the transient magnitudes observed with only the power or signal wiring connected. In

both of these cases, the magnitude of the signal wiring contribution was much greater than the power wiring contribution, and the frequency components of the transients observed on the complete system also closely matched those observed with the signal wiring only.

With Circuit 2, however, the transient magnitudes observed on the complete system were not a simple sum of the magnitudes observed in the other two cases. In fact, the magnitudes observed on the complete system were 30% less than those observed with only the power wiring connected. In this circuit, the predominant frequency in the transients observed on the complete system was 900 KHz, while this frequency component was not present at all in either case with the power or signal wiring connected separately.

The general conclusion to be drawn from the behavior of these circuits is that the coupling via the power and signal wiring is much more significant than the coupling directly into the NWDC, and that the relative importance of these two coupling mechanisms may be different for different circuits. In addition, the transient waveform observed on a complete system will not always be the sum of the contributions due to the signal and power wiring when acting separately.

5.3 Power-On Measurements

As described in paragraph 4.3, it was not possible to perform a comparison of the transients in the hard-wire and fiber optics configurations with power applied to the NWDC. It was also not possible to obtain a "clean" source of aircraft power; additional transient energy entered the aircraft during the power-on measurements via the

power cable. The observed power-on transients can therefore be expected to be greater in magnitude than those that might be experienced in flight, and they are slightly less meaningful in general than the power-off measurements.

Transient magnitudes measured on all circuits with power on were greater than the corresponding magnitudes measured with system power off. In the case of the power supply circuit, this increase was on the order of 300%. The transient magnitude increase in the three data circuits ranged from 300 to 600 per cent. Frequency content of the two other circuits remained essentially the same between power on and power off.

5.4 Electro-optical Circuits

Observations were made on Circuits 4 and 5 in order to establish the level of transient interference in the electro-optical circuits within the NWDC. Since these additional circuits do not exist when the NWDC is in the wire configuration, measurements could only be performed with the NWDC in the fiber optics configuration. For this reason, the observations on Circuits 4 and 5 cannot be considered in a comparison of fiber optics versus wires, and only serve to establish the level of transient interference in these circuits.

The transients observed within the electro-optical circuits were very low (less than 20 millivolts peak) and only twice the amplitude of the measurement system noise. Therefore, these circuits do not appear to be receiving large amounts of transient energy. The magnitude and frequency content of the signals observed were very similar to those observed on the data circuits with the system in the fiber optics configuration.

APPENDIX A

BASIC Language Software Listing

The following program is written in WDI TEK BASIC, the programming language used with the Tektronix Transient Digitizer system. It is included for reference purposes for those familiar with the language.

```
8000 PRINT "^[^L":PRINT "PROGRAM DATACQ.A74          27 AUG 76"
8005 GOSUB 9350:REMARK COMPUTE HANNING WINDOW.
8010 PRINT
8015 LET R7=7:PRINT "DATE: ";:INPUT DT:PRINT " "
8016 PRINT "CONFIG:";:INPUT CF:PRINT " ":PRINT "CKT ID:";:INPUT CK:PRINT
  " "
8017 PRINT "SENSOR, SCALE:";:INPUT S2,SF:PRINT " "
8018 PRINT "DATA TAPE NUMBER:";:INPUT TP:PRINT " "
8020 PRINT "ACQUIRE ZERO:  1-YES  2-NO  ";:INPUT X
8025 REMARK SENSORS:  1-IND VOLT, 2-IND CURRENT, 3-APPLIED CURRENT.
8030 IF X=2 THEN 8050
8040 ACQUIRE ZERO
8050 PRINT " ":PRINT "WAITING TO ARM.":WAIT
8070 DIGITIZE :PRINT "^G":ACQUIRE
8080 PRINT "1=GRAPH RAW  2=REZERO  4=REARM  ";:INPUT X1
8090 IF X1=2 THEN 8040
8100 IF X1=4 THEN 8070
8110 PRINT " ":PRINT "TIME:":INPUT T
8120 PRINT "^[^L":GRAPH RAW
8125 PLOT 0,0,780:GOSUB 9500
8130 PLOT 0,0,670:GOSUB 9550
8150 PRINT "TIME:":PRINT ;T:PRINT " "
8152 PRINT "CKT";CK:PRINT " "
8155 PRINT "TAPE";TP:PRINT " "
8160 PRINT "SCALE:":PRINT ;SF:PRINT " ":PRINT " "
8170 INPUT X1
8180 IF X1=2 THEN 8040
8190 IF X1=4 THEN 8070
8410 NORMALIZE A:LET A=A*SF
8420 LET HA=0:LET TA=0:LET VA=0:LET ZA=0
8425 LET HA$="S/DIV"
8430 IF S2=1 LET VA$="V/DIV":GOTO 8440
8432 LET VA$="A/DIV"
8435 IF S2>3 LET VA$="V/DIV"
```

```
8440 LET PP=MAX(A):LET PN=MIN(A)
8450 PRINT "^E^L":GRAPH A
8460 PLOT 0,0,780:GOSUB 9500
8464 PLOT 0,800,780:PRINT "^_MAX:";PP
8466 PLOT 0,800,740:PRINT "^_MIN:";PN
8470 PLOT 0,0,670:GOSUB 9550
8480 PRINT "TIME:":PRINT ;T:PRINT " "
8481 PRINT "CKT";CK:PRINT " "
8482 PRINT "TAPE";TP:PRINT " "
8485 PRINT "SCALE:":PRINT ;SF:PRINT " ":PRINT " "
8500 INPUT X1
8510 IF X1=2 THEN 8040
8520 IF X1=4 THEN 8070
8530 IF X1=5 THEN 9000
8540 IF X1=3 THEN 9070
8550 IF X1=6 THEN 8600
8553 IF X1=9 GOTO 8630
8555 IF X1=7 CREAD F,1,ALOFT,DT,T,CK,S2,CF,SF,PP,PN,TP,A,SA:GOTO 8450
8560 IF X1=8 GOTO 9400
8570 CWRITE 1,ALOFT,DT,T,CK,S2,CF,SF,PP,PN,TP,A,SA:GOTO 8500
8600 LET C=B*A*2.5:LET SC=SA
8601 REMARK WINDOWED WAVEFORM IN ARRAY C.
8605 FFT C,C,D,POLAR
8609 GOSUB 9600:REMARK CHANGE DISPLAY UNITS.
8610 LET HC$="HZ/DIV"
8620 LET TC=256:LET VC=0:LET ZC=0
8630 PRINT "^E^L":GRAPH C
8640 PLOT 0,0,780:PRINT "^_DATACQ.A74  CONFIGURATION";CF
8650 PLOT 0,450,780:PRINT "^_FFT MAGNITUDE SEQUENCE, RIGHT HALF PLANE."
8660 PLOT 0,120,710:PRINT "^_DC":PLOT 0,830,710:PRINT "^_";HC/1E+5;" MHZ
8670 PLOT 0,0,670:PRINT "^_INDUCED"
8672 IF S2=1 PRINT "VOLTAGE"
8674 IF S2=2 PRINT "CURRENT"
8676 PRINT " ":PRINT "CKT";CK:PRINT " "
```

```
8690 GOSUB 9550
8700 PRINT "TIME:":PRINT ;T:PRINT " ":PRINT " "
8710 GOSUB 9700:REMARK COMPUTE DOMINANT FREQUENCY.
8715 INPUT X1
8720 IF X1=2 THEN 8040
8722 IF X1=4 THEN 8070
8725 IF X1=1 THEN 8450
8730 IF X1=7 THEN 8555
8735 IF X1=5 THEN 9000
8740 PRINT " ":PRINT "EXPAND BY:";:INPUT X:LET HC=HC/X:GOTO 8630
9000 PRINT " ":PRINT "FILE SEARCH ON DRIVE 1.":PRINT ""
9015 PRINT "DATE, TIME:";:INPUT D2,T2
9020 CREAD F,1,ALOFT,DT,T
9030 IF DT<>D2 THEN 9020
9040 IF T<>T2 THEN 9020
9050 CREAD R,1,ALOFT,DT,T,CK,S2,CF,SF,PP,PN,TP,A,SA
9060 GOTO 8420
9070 PRINT " ":PRINT "HA,TA,VA,ZA:";:INPUT HA,TA,VA,ZA:GOTO 8450
9350 LET B=.6283:INTEGRATE B,B
9355 LET B=0.5*(1-COS(B)):LET B=B/MAX(B)
9365 RETURN
9400 LET B=0:LET SB=SA
9410 FOR J=0 TO 255
9415 LET I=J*2
9420 LET B(J)=(A(I)+A(I+1))/2
9425 NEXT J
9440 LET A=0:LET SA=SB*2
9460 FOR J=0 TO 255
9465 LET I=J+127
9470 LET A(I)=B(J)
9475 NEXT J
9490 GOTO 8420
9500 IF S2=1 PRINT "^_DATACQ.A74      INDUCED VOLTAGE      CONFIGURATION";
CF
9510 IF S2=2 PRINT "^_DATACQ.A74      INDUCED CURRENT      CONFIGURATION";
```

```
CF
9520 IF S2=3 PRINT "^_DATACQ.A74     APPLIED CURRENT     CONFIGURATION";
CF
9525 IF S2>3 PRINT "^_DATACQ.A74     SENSOR";S2;"     CONFIGURATION";CF
9530 RETURN
9550 IF DT>22 PRINT "^_DATE:":PRINT ;DT;" AUG":PRINT " "
9560 IF DT<23 PRINT "^_DATE:":PRINT ;DT;" SEPT":PRINT " "
9570 RETURN
9600 IF SC=1.024E+8 LET HC=5E+7
9605 IF SC=5.12E+7 LET HC=2E+7
9610 IF SC=2.56E+7 LET HC=1E+7
9615 IF SC=1.28E+7 LET HC=5E+6
9620 IF SC=1.024E+7 LET HC=5E+6
9625 IF SC=5.12E+6 LET HC=2E+6
9630 IF SC=2.56E+6 LET HC=1E+6
9635 IF SC=1.28E+6 LET HC=5E+5
9640 IF SC=1.024E+6 LET HC=5E+5
9645 IF SC=5.12E+5 LET HC=2E+5
9648 RETURN
9700 LET M=0
9705 FOR J=256 TO 350
9710 IF M<C(J) LET M=C(J):LET FM=J
9715 NEXT J
9720 LET FM=(FM-256)*SC/(51.2*1E+6)
9730 PLOT 0,925,670:PRINT "^_DOMINANT"
9735 PLOT 0,925,645:PRINT "^_FREQ:"
9740 PLOT 0,910,620:PRINT "^_";FM
9745 PLOT 0,0,400:PRINT "^_"
9750 RETURN
READY
*
```

END OF LISTING

☆U.S.Government Printing Office: 1977 — 757-001/103